DETERMINATION OF INDIUM BY VAPOUR GENERATION ATOMIC ABSORPTION SPECTROMETRY

A THESIS SUBMITTED TO
THE GRADUATE SCHOOL OF NATURAL AND APPLIED SCIENCES
OF
MIDDLE EAST TECHNICAL UNIVERSITY

BY

ERHAN ÖZDEMİR

IN PARTIAL FULFILLMENT OF THE REQUIREMENTS
FOR
THE DEGREE OF MASTER OF SCIENCE
IN
CHEMISTRY

JANUARY 2014

Approval of the Thesis;

DETERMINATION OF INDIUM BY VAPOUR GENERATION ATOMIC ABSORPTION SPECTROMETRY

Submitted by **ERHAN ÖZDEMİR** in a partial fulfillment of the requirements for the degree of **Master of Science in Chemistry Department, Middle East Technical University** by

Prof. Dr. Canan Özgen
Dean, Graduate School of **Natural and Applied Sciences** _____

Prof. Dr. İlker Özkan
Head of Department, **Chemistry** _____

Prof Dr. O. Yavuz Ataman
Supervisor, **Chemistry Department, METU** _____

Examining Committee Members:

Prof. Dr. İnci Gökmen
Chemistry Department, METU _____

Prof. Dr. Osman Yavuz Ataman
Chemistry Department, METU _____

Prof. Dr. Nusret Ertaş
Faculty of Pharmacy, Gazi University _____

Prof. Dr. Mürvet Volkan
Chemistry Department, METU _____

Prof. Dr. Semra Tuncel
Chemistry Department, METU _____

Date: 31.01.2014

I hereby declare that all information in this document has been obtained and presented in accordance with academic rules and ethical conduct. I also declare that, as required by these rules and conduct, I have fully cited and referenced all material and results that are not original to this work.

Name, Last name: Erhan Özdemir

Signature

ABSTRACT

DETERMINATION OF INDIUM BY VAPOUR GENERATION ATOMIC ABSORPTION SPECTROMETRY

Özdemir, Erhan

M.S., Department of Chemistry

Supervisor: Prof. Dr. O. Yavuz Ataman

January 2014, 91 pages

Determination of indium is important due to its growing importance in semiconductor industry and health concerns in occupational area. Due to extremely low abundance of indium in the earth crust, very sensitive and accurate methods are needed for its determination. Vapour generation atomic absorption spectrometry is a fast and economical technique for determination of conventional hydride generation elements such as As, Bi, Ge, Pb, Sb, Se, Sn, Te. However, there are very limited number of studies conducted for determination of indium by this method.

Continuous flow vapour generation system was set and parameters were optimized. 2.0 mol/L HCl was used to acidify the sample solution and 6.0% $NaBH_4$ was used for reduction of analyte to produce volatile species of indium. High memory effect, unstable nature of volatile species, unstable atomizer conditions were the problems affecting system performance.

To solve problems faced in continuous flow vapour generation system, a new design of flow injection vapour generation system was used. In this system, reaction coil was removed from conventional hydride generation systems in order to separate and transport volatile species rapidly. Moreover, this system was combined with a quartz atom trap to increase sensitivity. Quartz trap is based on consumption of hydrogen produced in reaction between carrier acid and reducing agent, with introduction of oxygen gas into the system. In the absence of hydrogen, atomization of volatile indium species is not realized and species are trapped on the surface of quartz tube atomizer. After optimizations, LOD and %RSD values were calculated as 41 μg/L and 4.9, respectively according to peak heights.

By removing parts of the system after saturation with 10.0 mg/L indium solution, sources of high memory problem of the system were investigated. It was concluded that adsorption on the GLS is the main source of memory effect.

Vapour generation efficiency was also investigated throughout this study. Waste solutions were picked up and analyzed in ETAAS instrument. It was concluded that vapour generation efficiency for indium was 10.5%.

Nature of volatile indium species was investigated. It was observed that indium volatile species can pass through 0.2 μm pore sized filter as it is in the case for stibine volatile species.

Photochemical vapour generation system was also designed and tested for indium. No achievement was gained in generation of volatile species using UV radiation and organic acid. Waste solutions were collected and analyzed in ICPOES to conclude that no indium volatile species were generated.

Keywords: Indium, vapour generation, quartz trap, memory effect, atomic absorption spectrometry

ÖZ

BUHAR OLUŞTURMALI ATOMİK ABSORPSİYON SPEKTROMETRE İLE İNDİYUM ELEMENTİNİN TAYİNİ

Özdemir, Erhan

Yüksek Lisans, Kimya Bölümü

Tez Yöneticisi: Prof. Dr. O. Yavuz Ataman

Ocak 2014, 91 sayfa

Yarı iletken endüstrisinde artan önemi ve özellikle çalışanların sağlığına verebileceği olumsuz etkileri sebebiyle indiyumun tayini önemlidir. İndiyum elementi doğada eser derişimlerde bulunduğu için tayininde duyarlı ve doğru sonuç veren metotlar kullanılmalıdır. Buhar oluşturmalı atomik absorpsiyon spektrometre As, Bi, Ge, Pb, Sb, Se, Sn ve Te gibi kolay hidrür bileşikleri oluşturan elementlerin tayini için hızlı ve ekonomik bir tekniktir. Fakat bu metodun indiyum tayini için kullanıldığı çalışmalar sınırlı sayıdadır.

Sürekli buhar oluşturmalı bir sistem geliştirilmiş ve parametreler optimize edilmiştir. Örnekler 2.0 mol/L HCl içinde hazırlanmış ve indiyumu indirgeyerek uçucu türler oluşturmak için % 6.0'lık $NaBH_4$ kullanılmıştır. Yüksek hafıza etkisi, uçucu indiyum türlerinin kararsız yapısı, kararsız atomlaştırıcı şartları sistem performansını etkileyen önemli parametreler olmuştur.

Sürekli buhar oluşturmalı sistemde karşılaşılan sorunların çözümü için yeni bir akışa enjeksiyon sistemi kullanılmıştır. Bu sistemde uçucu türlerin hızlı bir şekilde ayrılması ve taşınması için geleneksel hidrür oluşturma sistemlerinden

farklı olarak reaksiyon sarmalı kaldırılmıştır. Ek olarak sistem duyarlılığını artırmak için kuvars atom tuzağı kullanılmıştır. Kuvars tuzak, taşıyıcı asitle indirgeyici bileşiğin reaksiyonunda oluşan hidrojenin sisteme dışarıdan sağlanan oksijenle yakılarak tüketilmesine dayalıdır. Bu sayede hidrojenin yokluğunda uçucu indiyum türlerinin atomlaşması gerçekleşmediğinden bu türler kuvars tüpün yüzeyinde tutunmaktadır. Optimizasyonlarla birlikte, LOD ve %RSD değerleri, pik yükseklikleri temel alınarak 41 µg/L ve 4.9 olarak hesaplanmıştır.

Sistemin 10.0 mg/L indiyum çözeltisi kullanılarak doyurulmasından sonra bazı parçalarının sistemden çıkarılmasıyla yüksek hafıza etkisine neden olan bölümler tespit edilmiştir. GLS yüzeyinde tutunmanın hafıza etkisinin ana kaynağı olduğu saptanmıştır.

Buhar oluşturma verimi de bu çalışma kapsamında incelenmiştir. Sistemden toplanan atık çözeltileri ETAAS kullanılarak analiz edilmiş ve buhar oluşturma verimi indiyum için %10.5 olarak hesaplanmıştır.

İndiyum uçucu türlerinin nitelikleri de incelenmiştir. Uçucu indiyum türlerinin, antimon türlerinde de olduğu gibi gözenek boyutu 0.2 µm olan filtreden geçebildiği gözlemlenmiştir.

Fotokimyasal buhar oluşturma sistemi de kurulmuş ve indiyum için test edilmiştir. Organik asitte hazırlanan indiyum çözeltilerinin UV ışığına maruz bırakılmasıyla uçucu türlerin oluşturulması denenmiş fakat başarılı olunamamıştır. Bu aşamadan sonra atık çözeltileri toplanmış ve ICPOES kullanılarak analiz edilmiş ve indiyum uçucu türlerinin oluşturulamadığı sonucuna varılmıştır.

Anahtar Kelimeler: İndiyum, buhar oluşturma, kuvars tuzak, hafıza etkisi, atomik absorpsiyon spektrometre

To My Family; Sezin

ACKNOWLEDGEMENTS

I would like to express my sincere thanks to my supervisor Prof. Dr. O. Yavuz Ataman not only for his guidance, support, encouragement, patience and for teaching us how to become a good scientist but also for listening and helping us in many ways.

I would like to thank Assoc. Prof. Dr. Gülay Ertaş for her help and support throughout the study.

I would like to thank Assoc. Prof. Dr. Sezgin Bakırdere and Assist. Prof. Dr. Yasin Arslan for their ideas, constructive comments, moral support and their endless helps.

I am deeply grateful Pınar Akay, Emrah Yıldırım, Selin Bora and all C-49 and C-50 lab mates for their help, support and friendship.

I would like to thank Necati Koç for his help about technical issues.

I should also thank my friends Damla Şenlik and Yunus Erdal for their friendship and moral support.

Finally, my special thanks to my family and Sezin Atıcı for their trust, patience, support and love. I always know that they are with me and never leave me alone.

TABLE OF CONTENT

LIST OF TABLES

TABLES

LIST OF FIGURES

FIGURES

LIST OF ABRREVIATIONS

AAS	Atomic Absorption Spectrometry
AFS	Atomic Fluorescence Spectrometry
C_0	Characteristic Concentration
CHG	Chemical Hydride Generation
E	Enhancement Factor
ECHG	Electrochemical Hydride Generation
EHQTA	Externally Heated Quartz Tube Atomizer
ETAAS	Electrothermal Atomic Absorption Spectrometry
FAAS	Flame Atomic Absorption Spectrometry
GLS	Gas Liquid Separator
GTA	Graphite Tube Atomizer
HCL	Hollow Cathode Lamp
HG	Hydride Generation
HGAAS	Hydride Generation Atomic Absorption Spectrometry
HGAFS	Hydride Generation Atomic Fluorescence Spectrometry
HG-ETAAS	Hydride Generation Electrothermal Atomic Absorption Spectrometry

HG-IAT-AAS	Hydride Generation Integrated Atom Trap Atomic Absorption Spectrometry
ICPMS	Inductively Coupled Plasma Mass Spectrometry
ICPOES	Inductively Coupled Plasma Optical Emission Spectrometry
INAA	Instrumental Neutron Activation Analysis
ID	Inner Diameter
ITO	Indium Tin Oxide
LOD	Limit of Detection
LOQ	Limit of Quantification
NIOSH	National Institute for Occupational Safety and Health
PTFE	Polytetrafluoroethylene
QTA	Quartz Tube Atomizer
REL	Recommended Exposure Limit
RSD	Relative Standard Deviation
SQTAT-AAS	Slotted Quartz Tube Atom Trap Atomic Absorption Spectrometry
TLV	Threshold Limit Value
VGAAS	Vapor Generation Atomic Absorption Spectrometry

CHAPTER 1

INTRODUCTION

1.1 Indium

Indium is a p block element with the symbol In, atomic number of 49 and atomic mass of 114.818 amu. It has a melting point of 156.6 ^{o}C and boiling point of 2000 ^{o}C. It is a rare, very soft, silvery-white poor metal showing intermediate properties between gallium and thallium (Alfantazi & Moskalyk, 2003).

Indium was discovered by Ferdinand Reich and Hieronymus Richter in 1863 while testing ores from the mines around Freiberg, Saxony. They dissolved the minerals pyrite, arsenopyrite, galena and sphalerite in hydrochloric acid and distilled raw zinc chloride. From the indigo blue emission of this element, it was named as Indium **(**Reich & Richter**,** 1863**)**.

Indium is the 61st most abundant element in the Earth's crust by weight. It is found approximately 49 ppb in Earth's crust, and 0.0001 ppb in ocean water (Barbalace, 2013). There are fewer than 10 minerals of indium known. However, none of these occurs in significant deposits. Examples are the dzhalindite ($In(OH)_3$) and indite ($FeIn_2S_4$) (Sutherland, 1971).

There are two main oxidation states of indium, which are +1 and +3, with +3 being more stable. Indium (I) is reported as a powerful reducing agent (Bleshinsky & Abramova, 1958).

1.1.1 Occurrence and Production

Indium is created with the slow-neutron-capture process in the stars having a mass range of 0.6-1.0 mass of the Sun. When a silver-109 atom catches a neutron, it turns into a cadmium-110 with beta decay. By further neutron captures, it becomes cadmium-115, which decays to indium-115 (Boothroyd, 2006).

Indium is enriched in sulphide ores of lead, tin, copper, iron and zinc. Zinc production is the main source of indium. After leaching from the zinc tailings, indium is further purified with electrolysis. Average indium content of zinc deposits from which it is recovered ranges from less than 1 mg/kg to 100 mg/kg. (Tolcin, 2010) Canada is known to have the largest reserves of indium (Alfantazi & Moskalyk, 2003). The estimated reserves of indium in the world are approximately 40000 MT (Murphy & Mikolajczak, 2013).

China is a leading producer of indium, with a production of 390 tons in 2012. Canada, Japan and South Korea are the second, third and fourth leading producers, respectively. (Tolcin, 2013) Worldwide production of indium is 475 tons per year from mining and 650 tons per year from recycling. Indium production along the world between years 1972 to 2012 is given in Figure 1. (Murphy & Mikolajczak, 2013).

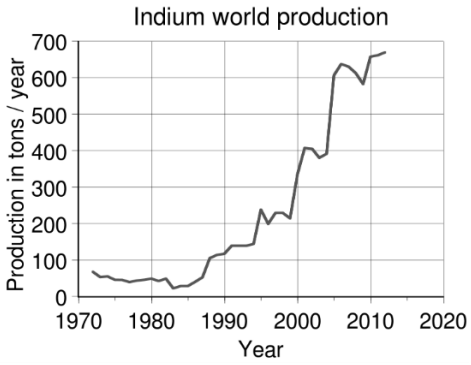

Figure 1: World indium production between years 1972 – 2012.

1.1.2 **Applications**

Indium tin oxide (ITO) is an n-type semiconductor which is widely used in solar panels, panel displays and LEDs as a transparent conductive electrode (Tadatsugu, 2005).

The use of InN finds application as semiconductors in optoelectronic devices, such as LEDs and lasers (Bhuiyan et al., 2003).

During World War II, indium was used as coating for bearings in high performance aircraft engines, leading to improved hardness, resistance to corrosion and anti-seizure properties.

Indium is used in the manufacture of low pressure sodium vapor lamps which are used for outdoor lighting. ITO is applied as a coating material which reflects infrared waves and transmits the visible light at the same time. This increases the operation temperature of the lamp, thereby increasing its efficiency (Downs, 1993)

Galinstan, which is an alloy of indium, gallium and tin is a replacement for mercury in liquid mirror telescopes for astronomy since it is less toxic than mercury and it has higher reflectivity and lower density.

A number of indium based solders are available having melting points down to 93°C. Moreover, indium is a minor addition to lead, bismuth and tin based solders (Virta, 2012).

Indium leukocyte imaging is a medical imaging technique which is used in early phase drug development and monitoring of white blood cells activity. In this technique, white cells labeled with ^{111}In, which emit gamma radiation, are injected to the patient. White cell localization is then monitored with gamma imaging, which gives information about areas of infection (Nostrand, Abreu, Callaghan, Atkins, Stoops, & Savory, 1988).

1.1.3 Indium and Metabolism

There is no report in the literature about any toxic effects of metallic indium. Exposure to indium compounds is usually by inhalation. Clearance of both soluble and insoluble indium compounds is slow. After chronic exposure, indium is reported as accumulating in the lungs (Hoet et al., 2012). Indium is transported to the blood with transferrin and accumulated in kidney. Soluble and insoluble indium compounds are removed from the body with urine and feces (Zheng et al., 1994).

Inflammations, alveolar proteinosis, interstitial fibrotic changes after inhalational exposure to ITO were reported in the animal studies. Repeated inhalational exposure to ITO at or below 0.1 mg/m^3 was reported as increasing malignant lung tumors in rats (Nagano et al., 2011).

There are several studies conducted on health effect of indium phosphide (InP) to mice and rats. Lung tumors and benign incidents are reported to be increased with increasing time of exposure. Alveolar proteinosis, alveolar/bronchiolar adenomas were also reported (Gottschling et al., 2001). Testicular damage has also been reported in a research conducted on hamsters (Omura et al., 2000).

Up until now, there are six case reports on effect of inhaled indium compounds on humans. In one case, a worker was died of bilateral pneumothorax. Tin and indium were detected by X-ray analyzer on the particles found in his lung and the particles were decided to be ITO. Indium concentration in his serum was found to be 290 μg/L (Homma et al., 2003). Another worker, who developed pulmonary fibrosis and emphysema during his 4-year exposure to indium tin oxide, showed no progression of the disease after leaving his work related to indium (Homma et al., 2005). Case reports were summarized in Table 1 (Tanaka et al., 2010).

Table 1: Published case reports of interstitial pneumonia caused by inhaled indium compounds.

Reference	Case Age	Duration of engagement	Serum indium level (μg/L)
(Homma, Ueno, Sekizawa, Tanaka, & Hirata, 2003)	27	3	290
(Hosseini, Chamsaz, Raissi, & Naseri, 2005)	30	4	51
(Taguchi & Chonan, 2006)	31	12	40
(Taguchi & Chonan, 2006)	39	12	127
(Taguchi & Chonan, 2006)	28	8	99
(Taguchi & Chonan, 2006)	43	5	65

Recommended exposure limit (REL) of National Institute for Occupational Safety and Health (NIOSH) and Threshold Limit Value (TLV®) of American Conference of Governmental Industrial Hygienists for indium and indium compounds is 0.1 mg/m^3 (ACGIH, 2001).

1.1.4 Determination of Indium

Since concentration of indium is very low in real samples, like metal ores, geological samples etc., conventional methods such as Flame Atomic Absorption Spectrometry (FAAS) and Inductively Coupled Plasma Optical Emission Spectrometry are not always suitable for determination of indium in real samples. Thus several methods have been conducted in the literature for determination of indium including Hydride Generation Atomic Absorption Spectrometry (HGAAS), Hydride Generation - Integrated Atom Trap Atomic Absorption Spectrometry (HG-IAT-AAS), Hydride Generation - Electrothermal Atomic Absorption Spectrometry (HG-ETAAS), Slotted Quartz Tube Atom Trap Atomic Absorption Spectrometry (SQTAT-AAS), Electrothermal Atomic Absorption Spectrometry (ETAAS) and Inductively Coupled Plasma Mass Spectrometry (ICPMS).

All authors studying chemical hydride generation of indium noted low reaction yields for indium. Possible causes of this low yields can be unstable nature of volatile indium compounds and kinetic problems with hydride formation. Moreover, atomization of possible indium volatile compounds may not be as straightforward as it is in other conventional hydride generation elements (Dědina & Tsalev, 1995).

Busheina and Headridge (Busheina & Headridge, 1982) applied Hydride Generation and Atomic Absorption Spectrometry with a batch system connected to an electrically heated atomizer in 1982 and reported a characteristic mass of 0.3 µg and characteristic concentration of 0.5 mg/L. Schematic representation of the study is illustrated in Figure 2.

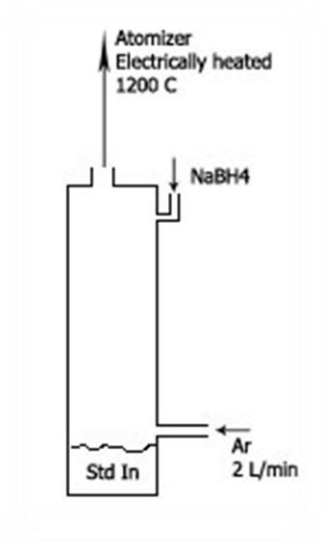

Figure 2: Schematic representation of the study conducted by Busheina and Headridge (Busheina & Headridge, 1982).

Yan et al. (1984) prepared a batch system at 60 °C reaction temperature for determination of indium with HGAAS. They reported a characteristic mass of 0.13 µg with 8.5% precision for 10 readings in terms of RSD.

In 1993, Liao & Li (Li & Liao, 1993), also set up a batch hydride generation system for determination of indium with ETAAS. In that system, generated hydrides at 60 °C were transported to a palladium coated graphite furnace and after a certain collection period, atomization was realized at 2300 °C. With the system, they reached a 0.63 ng characteristic mass for *in-situ* preconcentration of volatile compounds generated and 0.011 ng characteristic mass for direct sampled indium standard solution. The study is illustrated schematically in Figure 3.

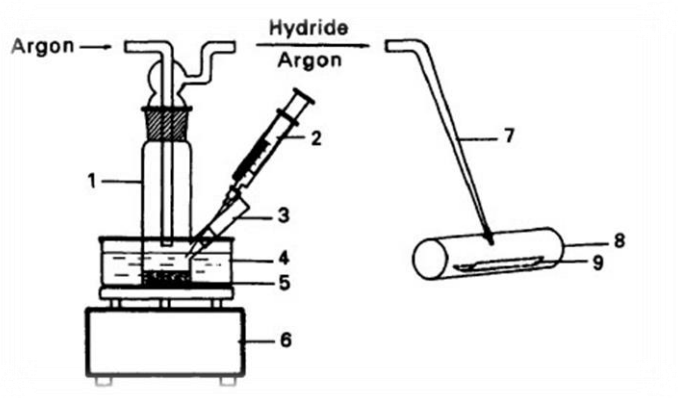

Figure 3: Schematic representation of the study conducted by Liao and Li. (Li & Liao, 1993).
1, glass hydride generator; 2, syringe; 3, PTFE tube; 4, hot water-bath; 5, magneton; 6, electromagnetic stirrer with heating set; 7, quartz capillary tube; 8, pyrolytic graphite coated graphite tube; and 9, pyrolytic graphite coated graphite platform.

Matusiewicz (Matusiewicz & Krawczyk, 2007) prepared HG-ETAAS, IAT-FAAS and HG-IAT-FAAS systems for determination of indium and reported 6.3, 10.0 and 0.60 μg/L detection limit, respectively, with 3s blank criterion for 6 replicate measurements.

Arslan et al. (2011) designed an SQT-FAAS and SQT-AT-FAAS method for indium determination and reported a detection limit of 600 μg/L and 2.60 μg/L, respectively. Within the scope of that study, they examined the nature of the trapped indium volatile compounds on the quartz surface with XPS and reported that oxidation state of indium trapped on the quartz surface was +3.

1.2 Atomic Absorption Spectrometry (AAS)

Optical spectroscopy began with the observation of Sir Isaac Newton that sunlight splits into several colors when it is passed through prism. From that time on, numerous experiments were performed in order to understand the nature of light. Scientists understood the close relation of light and matter after the black lines in the spectrum of sun were noticed by Wollaston in 1802.

Principle of absorption and dark lines in spectrum of sun were firstly explained by Bunsen and Kirchhoff. They concluded that matter absorbs light in certain wavelengths, in which it also emits light. Hollow cathode lamps were developed by Sir Alan Walsh at the Commonwealth Scientific and Industrial Research Organization (CSIRO). First AAS instruments were developed by this team during the 1950s (L'vov, 2005).

AAS is based on absorption of electromagnetic radiation which is delivered from a hollow cathode lamp (HCL) specific to the analyte, which is vaporized through the optical path of the spectrometer and then atomized there. Energy difference between the ground and excited state of the analyte determines the wavelength of the absorbed light. Light from the radiation source is basically delivered to the detector through an atomization unit and a wavelength selection unit. Block diagram of AAS is illustrated in Figure 4.

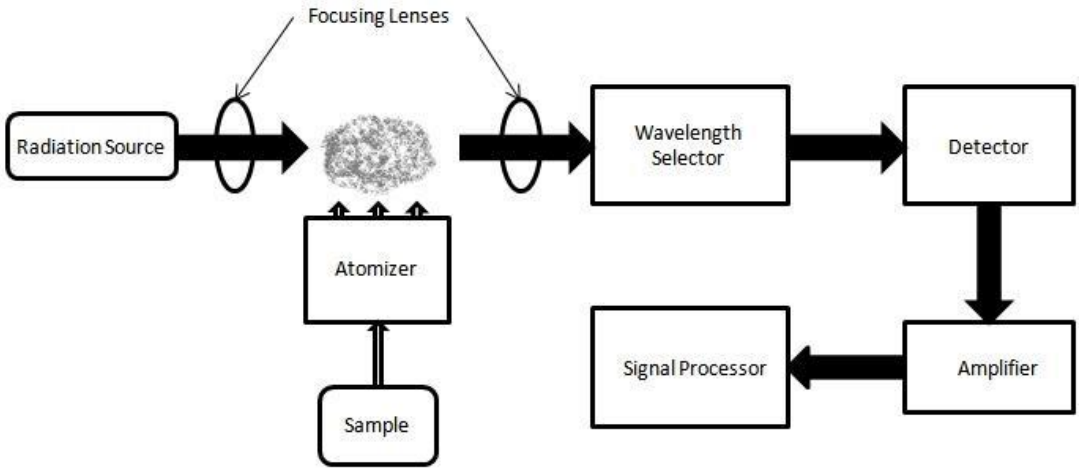

Figure 4: Block diagram of an Atomic Absorption Spectrometer (Wikipedia, 2008).

AAS is the most popular atomic spectrometry method since it is robust, well established and cheapest in terms of running costs (Dědina, 2010).

AAS can be classified as Flame AAS (FAAS) and Electrothermal AAS (ETAAS) based on its atomization unit.

1.2.1 Flame Atomic Absorption Spectrometry (FAAS)

In flame AAS, analyte solution is converted into aerosol in nebulizer and transported into the atomization unit, which is a flame. Vaporization and atomization of the analyte is realized inside the flame. Chemical composition of the flame is important in determining the performance of the flame. Acetylene is typically used as fuel and air as oxidant in AAS. Alternatively, hydrogen, propane/butane can be used as fuel. Other oxidant alternatives are O_2 and N_2O. Maximum temperature of a standard air-acetylene flame is 2250 °C and maximum burning velocity is 158 cm/s (Welz & Sperling, 1999).

In FAAS, sample solution is introduced inside the flame with the help of a nebulizer. With the passage of oxidant, a partial vacuum is produced (ventury effect) and

aerosol is produced with different sizes of droplets. Aerosol, oxidant and fuel are mixed in a chamber and enter the flame.

Flame AAS is inexpensive, simple and durable. Also, with the fuel and oxidant alternatives, temperature of the flame can be varied for optimum conditions. However, flame AAS has some disadvantages. Nebulizers are only 10% efficient at most for introduction of the sample. Moreover, analyte aspirated to the flame have a very short residence time in the measurement zone, making the sample consumption high. Also, solid sampling is not possible and nebulization of viscous liquids may not be achieved with the nebulizer systems in FAAS. Self-absorption of the flame components and emission at the analyte's wavelength are sources of possible interference in FAAS technique. In addition, density of the analyte atoms in the flame is limited due to high volume of fuel and oxidant gas and also flame gas expansion during combustion in the measurement zone (Cantle, 1982).

1.2.2 Electrothermal Atomic Absorption Spectrometry (ETAAS)

Dilution of the analyte in the measurement zone in FAAS can be avoided with introducing the sample directly on the measurement zone. In ETAAS, a very small amount of sample is placed inside a graphite tube or metallic tube. Vaporization and atomization of the analyte occurs inside the tube with resistively heating, making the residence time longer and density of the analyte atoms higher compared to FAAS (Broekaert, 2005).

With this method, chemical environment can also be controlled in a certain extent supplying inert atmosphere with introduction of Ar or N_2 inside the tube. Temperatre inside the tube is controlled with differing the voltages on the ends of the graphite tube. For melting solid samples, drying liquid samples, partially or fully removing the matrix, modifying the matrix and enhancing the atomization, atomization of the analyte and cleaning the tube, temperature is increased with a step by step program.

With these inherent advantages of the ETAAS, a 1000-fold increase in the sensitivity can be achieved compared to FAAS (Cantle, 1982).

Despite its advantages, ETAAS has some disadvantages, too. Interferences may be faced if the matrix cannot be modified or removed with the help of temperature program and purge gas. Additionally, temperature profile of the graphite tube is not homogenous, making the atomization inhomogeneous. Different forms of the analyte can be present inside the graphite tube resulting in splitted or distorted peaks (Frech & Baxter, 1995). Contamination of the tube from one analysis to the second one can be also faced at ultra-trace levels (Cantle, 1982).

1.3 Vapor Generation Atomic Absorption Spectrometry (VGAAS)

Due to the low transport efficiency of FAAS, alternative methods for sample introduction are being searched. Chemical properties of some elements are suitable for converting them to a volatile elemental or molecular form. This conversion allows these elements to be separated from the liquid matrix before introduction into the measurement zone. With or without the help of a carrier gas, the volatile species are introduced to the optical path of the AAS instrument. With this process, interferences resulted from the high matrix may be minimized (Dědina & Tsalev, 1995).

Generation of volatile species can be achieved by generation of hydride (Gonzalvez et al., 2009), cold vapor (Liva et al., 2000), chelate (Leskela et al., 1991), alkyl (Chau et al., 1982), carbonyl (Johansson et al., 1998), oxide (Gregorie, 1990), and halide (Skogerboe et al., 1975). Analytes and techniques appropriate for volatile species generation are summarized in Table 2.

Table 2 Summary of Chemical Vapor Generation Methods in AAS (Tsalev, 1999)

Chemical system for vapour generation	Analyte[a]
Hydride generation (HG)	***As***, ***Bi***, ***Ge***, (In), Pb, ***Sb***, ***Se***, ***Sn***, ***Te***, (Tl)
Cold vapour (CV) technique	Cd, ***Hg***, (Cu?)
Ethylation	Bi, Cd, Co, Ge, ***Hg***, ***Pb***, ***Se***, ***Sn***, Tl
Butylation	Be, Ga, ***Hg***, ***Pb***, ***Sn***, Zn
Carbonyl generation	Co, Fe, ***Ni***
Chlorides	As, Bi, Cd, Ge, Mo, Pb, Sn, Tl, Zn
Fluorides	Ge, Mo, Re, U, V, W
Dithiocarbamates	Co, Cr, Cu
β-Diketonates	Al, Co, Cr, Cu, Fe, Mn, Ni, Pb, Zn
Miscellaneous VG techniques	***$B(CH_3O)_3$***, OsO_4

[a]Species in bold itallic indicate straightforward analytical performance; Species in parantheses indicate serious problems with that particular analyte.

1.3.1 Hydride Generation Atomic Absorption Spectrometry (HGAAS)

Hydride Generation AAS involves two separate processes, such as generation of the hydride and atomization of the hydride.

Elements including Sb, As, Bi, Ge, Se, Te, and Sn readily form volatile hydrides upon the reduction of the analyte in an acidified solution with a reducing agent, such as sodium borohydride. The volatile hydride produced is transported to the atomization unit by the help of a carrier gas such as Ar, N_2 or air (Cantle, 1982). Common hydride forming elements and physical properties of their hydrides are summarized in Table 3.

Table 3: Physical properties of hydrides (Dedina & Tsalev, 1995)

Element	Name	Formula	Melting Point, °C	Boiling Point, °C	Solubility in Water (µg/mL)
As	Arsine	AsH_3	-116.3	-62.4	696
Bi	Bismuthine	BiH_3	-67	16.8	-
Ge	Germane	GeH_4	-164.8	-88.4	Insoluble
Pb	Plumbane	PbH_4	-135	-13	-
Sb	Stibine	SbH_3	-88	-18.4	4100
Se	Hydrogen Selenide	H_2Se	-65.7	-41.3	37700-68000
Sn	Stannane	SnH_4	-146	-52.5	-
Te	Tellurium Hydride	H_2Te	-51	-4	Very Soluble

Generation of the hydride can be achieved either chemically or electrochemically. In chemical hydride generation, a chemical reaction is employed between acidified analyte and a reductant, forming a hydride of the analyte.

At the beginning, mechanism of the hydride generation reaction was explained with nascent hydrogen mechanism. According to this mechanism, it is assumed that BH_4^- is decomposed in an acidic media, producing nascent hydrogen. After the decomposition is complete, the analyte is reduced with the resulting nascent hydrogen (Robbins & Caruso, 1979).

$$BH_4^- + H^+ + 3H_2O \rightarrow H_3BO_3 + 8H$$

$$A^{m+} + (m+n)\,H \rightarrow AH_n + mH^+$$

Nascent hydrogen model was never proved. However it was accepted until D'ulivo et al. (2005) studied the mechanism by labeling the BH_4^- species with deuterium. In the study with Bi, they verified that direct transfer of hydrogen bonded to boron occurred. With this study, they expressed an alternative "hydrogen-transfer" theory.

According to the hydrogen-transfer theory, mechanism of hydride generation consists of two steps. In the first stage, BH_4^- is hydrolyzed stepwise to H_3BO_3. As a result of low reaction rates, there are four hydroboron species in the reaction mixture.

$$BH_4^- \rightarrow H_2O\text{-}BH_3 \rightarrow H_2O\text{-}BH_2OH \rightarrow H_2O\text{-}BH(OH)_2 \rightarrow H_3BO_3$$

In the second stage, hydrogen transfer from one of these hydroboron species to the analyte occurs in a stepwise process (Dědina, 2010).

In spite of its advantages, chemical hydride generations have also some disadvantages. Consumption of high amounts of $NaBH_4$ makes the method expensive and also more prone to interferences. High blanks are mainly due to $NaBH_4$ (Menemenlioğlu et al., 2007). In addition, $NaBH_4$ is not easy to handle since it is not stable. It decomposes with a surface catalyzed process and it can not be stored for a long time (Dědina & Tsalev, 1995). Electrochemical hydride generation is one alternative to the chemical hydride generation. In this method, electric current is employed rather than reducing agents for reduction of the analyte. Water and

hydronium ions are reduced to hydrogen in the cathode and water is oxidized to oxygen in the anode. Hydride is formed on the cathode surface and separated from the solution (Laborda et al., 2007).

1.3.2 Photochemical Vapour Generation (PVG)

Generation of volatile compound of many elements can be achieved by exposing the analyte to UV radiation in the presence of a low molecular weight acid. First study on the UV irradiation was conducted by Xuming et. al. for determination of Se. Inorganic selenium was converted into hydride, carbonyl and methyl compounds by irradiation with mercury lamp at 254 nm in formic, acetic, propionic and malonic acids (Xuming et al., 2003). The mechanism of the vapour generation by photochemical reaction was not fully explained. Experimental set-up of a photochemical vapor generation system is illustrated in Figure 5.

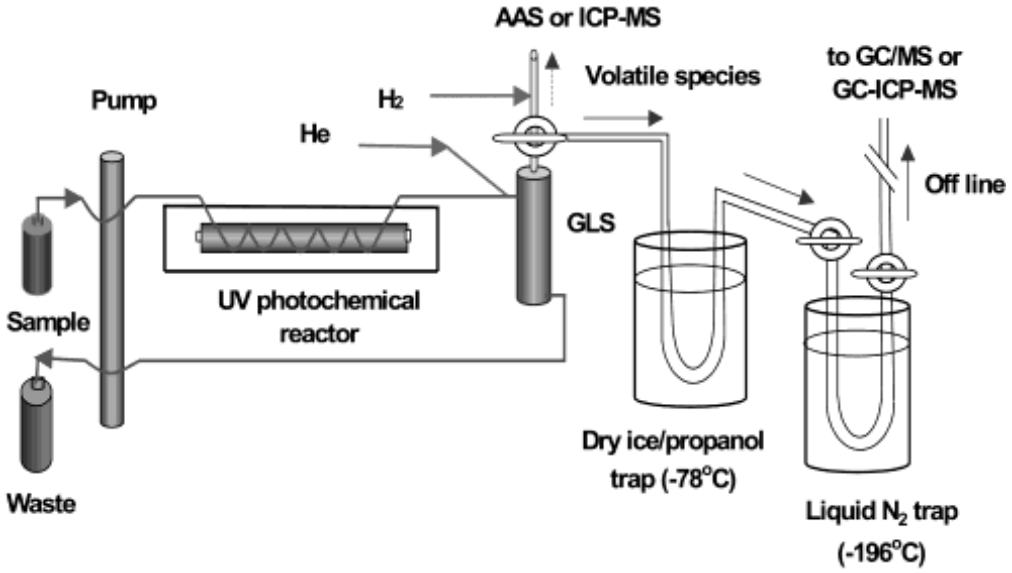

Figure 5: Schematic diagram of an experimental set-up for PVG (Xuming et al., 2003)**.**

1.4 Hydride Atomization

The final step in vapor generation methods is atomization of the volatile species transported into the measurement zone. There are several designs for atomization of hydrides in order to fulfill the criteria of an ideal atomizer. In an ideal atomizer, analyte must be converted to free atoms completely and no reaction of free atoms must take place in the measurement zone. Longer residence time of the free atoms in the optical path is another important issue which is necessary for high sensitivity. In order to achieve a lower detection limit, an ideal atomizer should not make a contribution to measurement noise. Moreover, an ideal atomizer should be suitable for possible preconcentration techniques, should be robust and be available with low running costs.

1.4.1 Inert Gas – Hydrogen Diffusion Flames

Introduction of hydrides to the flame atomizer suffers from short residence time and high atomizer noise. Thus it is unprofitable to use conventional burner for hydride atomization. Ebdon et al. (1982) improved the residence time using an argon/hydrogen flame on the top of a small quartz tube with 8.5 mm inner diameter. Thanks to the lower gas flow rates in the tube, residence time can be increased. Hydrogen radicals are formed in the flame protecting and isolating free analyte atoms from chemical reactions with oxygen and other species. In addition, it's a very simple to set-up and has low building cost. However, sensitivity is low, with 30-60 times greater LOD compared to quartz tube atomizers. A miniature diffusion flame is represented in Figure 6.

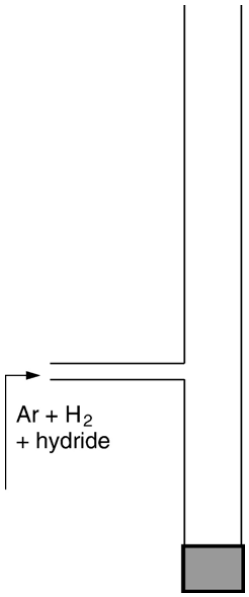

Figure 6: Schematic representation of a miniature diffusion flame (Dědina, 2010).

1.4.2 Externally Heated Quartz Tubes (EHQTA)

These type of atomizers are simply L or T-shaped quartz tubes. Horizontal arm of the tubes was aligned on the optical arm of the spectrometer. Inlet arm is used for introduction of volatile species. Air acetylene flame or resistively heated furnaces can be used in order to reach the atomization temperature inside the tube.

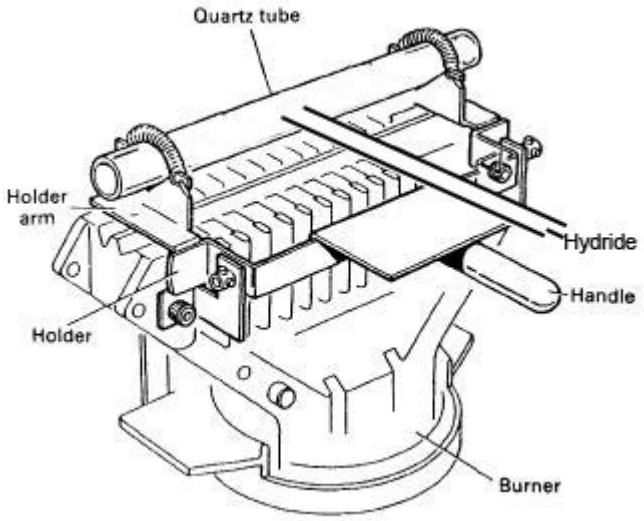

Figure 7: Schematic representation of a QTA (Welz & Sperling, 1999).

With the use of quartz tube atomizers, residence time of free atoms is increased. This brings the advantage of higher sensitivity. A small fraction of hydrogen is required inside the tube in order to create an atmosphere with hydrogen radicals since hydride atomization requires hydrogen radicals. No free analyte atoms are observed in the absence of hydrogen radicals (Dědina, 2010). This hydrogen is supplied from the reaction between tetrahydroborate and acid reaction. Different from diffusion flames, outer flow of oxygen is not employed in QTA. A small amount of oxygen to form a hydrogen-oxygen flame and hydrogen radical cloud inside is needed. Oxygen present

in the air, inside the QTA and inside the sample and carrier gas is usually enough for production of a hydrogen radical cloud.

1.5 Multiple Microflame Quartz Tube Atomizer (MMQTA)

Longer residence time is an important advantage of quartz tube atomizers. However, hydrogen cloud covers only a small portion of the QTA and free atoms are stable only inside the hydrogen cloud. Dedina and Matousek (Dedina & Matousek, 2000) improved the QTA with a design called multiple microflame QTA. In this design, another quartz tube is used to cover the optical arm of the QTA. From the space between the two tubes, oxygen is introduced. Inner tube contains regularly distributed tiny orifices allowing the passage of oxygen inside the inner tube. Microflames are formed on the holes with the oxygen gas present and hydrogen supplied from the reaction of THB-acid reaction. With this design, microflames and thus hydrogen radical clouds are distributed over the optical arm of the QTA, making the free analytes more stable and resistant to interferences over a longer path. Schematic representation of MMQTA is shown in Figure 8.

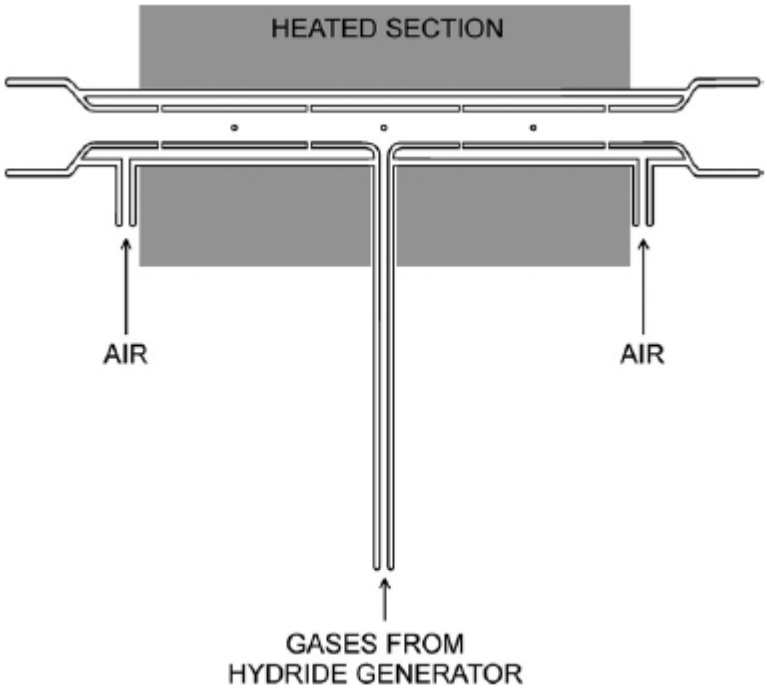

Figure 8: Schematic representation of MMQTA (Dedina & Matousek, 2000).

1.6 Quartz Atom Traps

In order to enhance sensitivity of the vapor generation systems, they can be engaged to various trapping procedures, which includes preconcentration of the volatile species on the surface of a trapping medium. Trapping medium can be surface of the graphite cuvette, crushed silica or surface of the quartz atomizers and metal surfaces coated or uncoated with several elements.

The idea of quartz atom trap coupled with chemical conventional hydride generation system was used in the study conducted by Korkmaz and her co-workers. In their study, three pieces of crushed quartz tube were inserted into a cylindirical quartz tube and positioned after the junction point of inlet arm and optical arms of QTA. This trapping system was heated externally by the help of a nickel-chromium wire.

Volatile species of Pb were trapped at 500 °C for a certain time and the quartz trap was heated furher to 900 °C for revolatilization of trapped species (Korkmaz et al., 2002). This trapping system was also applied successfully to hydride generation of Sb (Korkmaz et al., 2004), cold vapor generation of Cd (Korkmaz et al., 2005) and electrochemical hydride generation of Sb (Menemenlioğlu et al., 2007). Scheme of the hydride generation system combined with quartz trap is shown in Figure 9.

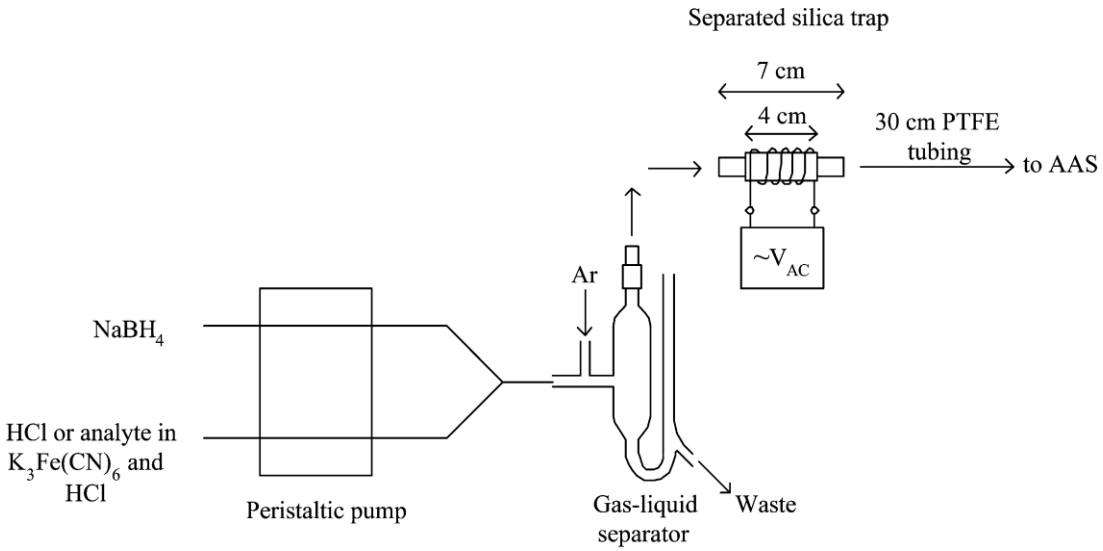

Figure 9: Schematic representation of continous flow VG system coupled with quartz trap (Korkmaz et al., 2002).

Kratzer and Dedina used the surface of QTA as trapping medium in their study conducted for determination of Bi. They placed a quartz capillary tube inside the inlet arm of QTA for introduction of oxygen. Aim of oxygen introduction was to make a combustion reaction between oxygen from an external source and hydrogen which was released from the reaction between THB and acid. In the trapping step oxygen was introduced into the inlet arm and volatile species were trapped on the

surface of QTA in the absence of hydrogen. When oxygen introduction was stopped, atomization is realized (Kratzer & Dedina, 2005).

1.7 Purpose of the Study

As a result of increasing demand for indium in semiconductor industry and health concerns associated with indium compounds in recent years; sensitive, robust and inexpensive methods for determination of indium becomes a more important issue in the occupational area. Proposed methods in the literature for determination of indium generally suffer from low sensitivity and high costs. The main purpose of this study is to offer a sensitive and low-cost analytical technique for determination of indium. For this purpose, flow injection vapor generation atomic absorption technique will be coupled with a quartz trap. Optimizations of parameters will be held in flow injection vapor generation system and reproducible signals will be gained with a satisfying detection limit. In this system, vapor generation efficiency of indium and also the behavior of the volatile species of indium in quartz trap will be investigated. Another purpose in this study is to examine the nature of the volatile species. Although transported analyte species are frequently called “volatile”, previous studies have shown that in some cases analyte is carried in the form of nanoparticles. Examples for these type of analytes include Au (Arslan et al., 2011), Ag (Musil et al., 2011) and Tl (Ataman, 2011). Similar studies will be carried out for In. Moreover, molecular information of the trapped indium species will be investigated.

CHAPTER 2

EXPERIMENTAL

2.1 Chemicals and Reagents

All reagents used throughout the studies were of analytical grade or higher purity. A 50 mg/L intermediate stock solution of indium was prepared in 0.47 mol/L HCl from a 1000 mg/L stock solution (High Purity Standards) of indium which was prepared from In metal in 2% HNO_3 (v/v). All the working indium standard solutions were prepared in 0.47 mol/L HCl with necessary dilutions of 50.0 mg/L intermediate stock solution. A 1000 mg/L Pd stock solution was prepared by dissolving solid $K_2(PdCl_6)$ (Aldrich) in 10% (v/v) HNO_3. Stock solution of 0.1% (w/v) rhodamine B (Allied Chemical, Morristown), 0.1% (w/v) 8-hydroxy quinoline (Merck), 0.1% dithizone (Merck), 0.1% Rhodamine 6G (AppliChem) and 0.1% 8-mercapto quinoline (TCI) were prepared in deionized water and all are stored in refrigerator. Solutions were diluted using 18 MΩ·cm deionized water obtained from TKA (Thermo Scientific, Stockland, Germany) Pacific PW reverse osmosis water purification system. Acidification of standard solutions was made using analytical grade 37% (w/w) HCl (Merck, Germany).

Powdered proanalysis grade $NaBH_4$ (Merck, Darmstadt, Germany) was used in order to prepare 3% (w/v) of reductant solution in 0.3% (w/v) NaOH (Merck). Solution was not filtered before using.

Throughout the study, high purity Ar (99.999 %), high purity O_2 (99.999 %) and high purity H_2 (99.999 %) gases were used (Linde Gaz, Ankara, Turkey).

All the glass and plastic apparatus were kept in 10% (v/v) HNO_3 and rinsed with deionized water before use so as to minimize possible contaminations.

2.2 Instrumentation

2.2.1 Atomic Absorption Spectrometer

For continuous flow vapor generation studies, an ATI Unicam 929 atomic absorption spectrometer was used. For flow injection VCG studies, a Varian AA140 (Victoria, Australia) atomic absorption spectrometer was used. Both instruments were equipped with a deuterium arc background correction system and 10.0 cm burner head. Data were processed by SpectrAA software (version 5.1). A Philips coded In hollow cathode lamp was used as a radiation source for 303.9 nm indium line. Instrumental parameters are summarized in Table 4.

Table 4: Operating conditions of AA spectrometer

Parameter	Value
Measurement Wavelength, nm	303.9
Spectral bandpass, nm	0.5
Lamp Current, mA	5
Flame Type	-
Read Time, s	10
Measurement mode	Peak Height

2.2.2 Electrothermal Atomic Absorption Spectrometer

Electrothermal atomic absorption studies were performed using a Varian GTA 120 graphite tube atomizer unit. 10.0 µL of sample solutions were injected with 5.0 µL of 1000 mg/L Pd as modifier. 325.6 nm was selected as the wavelength. Temperature program in the graphite furnace was summarized in Table 5.

Table 5: Temperature program of ETAAS system used in efficiency study

Step	Temperature, ºC	Ramp time, s	Ar flow, L/min
1	85	5.0	0.3
2	120	40.0	0.3
2	120	10.0	0.3
3	600	5.0	0.3
5	2700	1.3	0
6	2700	2.0	0.3

2.2.3 Inductively Coupled Plasma Optical Emission Spectrometer

Throughout the waste analysis of UV photochemical vapor generation studies, a Leeman Labs Inc. Direct Reading Echelle ICP-OES instrument was used with axial view configuration. 325.6 nm was selected as reading wavelength for indium determination. Instrumental parameters of ICP-OES are summarized in Table 6.

Table 6: Operating conditions of ICP-OES instrument used in waste analysis of UV PVG study.

Parameter	Value
Power, kW	1.2
Frequency, MHz	40
Coolant gas flow rate, L/min	19
Auxiliary gas flow rate, L/min	0.5
Nebulizer pressure, PSI	35
Sample flow rate, mL/min	0.5

2.2.4 Raman Spectrometer

Vibrational spectrometry studies for seeking molecular information of trapped indium species were performed using a Bruker Senterra Confocal Raman Spectrometer with 1-3 cm^{-1} resolution and 532 nm excitation wavelength. The instrument was equipped with 50x lens.

2.2.5 X-Ray Diffraction Spectrometer

Qualitative analysis of trapped indium species were also performed by the help of a Rigaku Miniflex X-Ray Diffraction instrument equipped with a Miniflex goniometer, 30kV/15mA X-Ray source and a standard sample holder. Scannings were held in 2theta/theta mode with continuous scanning.

Throughout the flow injection studies, a lab-made resistively heated cylindrical ceramic furnace to accommodate a QTA with 1.8 cm outer diameter and 14 cm width was used in order to achieve the atomization temperature. The heater consists of two semi-cylindrical ceramics that can cover top and bottom of the horizontal arm of the quartz T-tube atomizer. Ceramic part was covered with quartz wool and placed inside an aluminum box. In order to control the temperature of the heater, a GEMO DT109 temperature controller (Gürbüzoğlu Elektronik, Ankara, Turkey) was coupled with the heater. A thermocouple was placed inside the bottom semi-cylindrical part of the ceramic in order to measure the temperature. A picture of the heating unit is shown in Figure 10.

Figure 10: Lab-made ceramic electrical heater used to heat QTA to atomization temperature.

2.3 Vapor Generation System

Experiments were performed in continuous and flow injection mode. Yellow-blue color coded 1.27 mm id Tygon® peristaltic pump tubing were used in order to send the sample solution and reductant $NaBH_4$ solution to the gas-liquid separator. Constant flow rates are achieved by the help of Gilson Minipuls 3 (Villers Le Bell, France) 4-channel peristaltic pumps. Waste solution is removed from the system by Gilson Minipuls 3 peristaltic pumps.

For the junction points of tubing and carrier gas, 3 way Y-shaped PTFE connectors (Cole Palmer, Illinois, USA) were used.

High purity argon was introduced into the system for stripping of the formed hydrides from sample solution by the help of PTFE flow meters (Cole Palmer). Flow meters were calibrated regularly by a laboratory made soap bubble flow meter.

Throughout the study, an externally heated quartz T-tube atomizer (QTA) was used. By the help of a support device, optical arm of the QTA was placed above the spray chamber. Every new QTA was saturated with 100 mL of 2.0 mg/L In standard solution before use by the optimized vapor generation procedure. Schematic representation and dimensions of the QTA is shown in Figure 11.

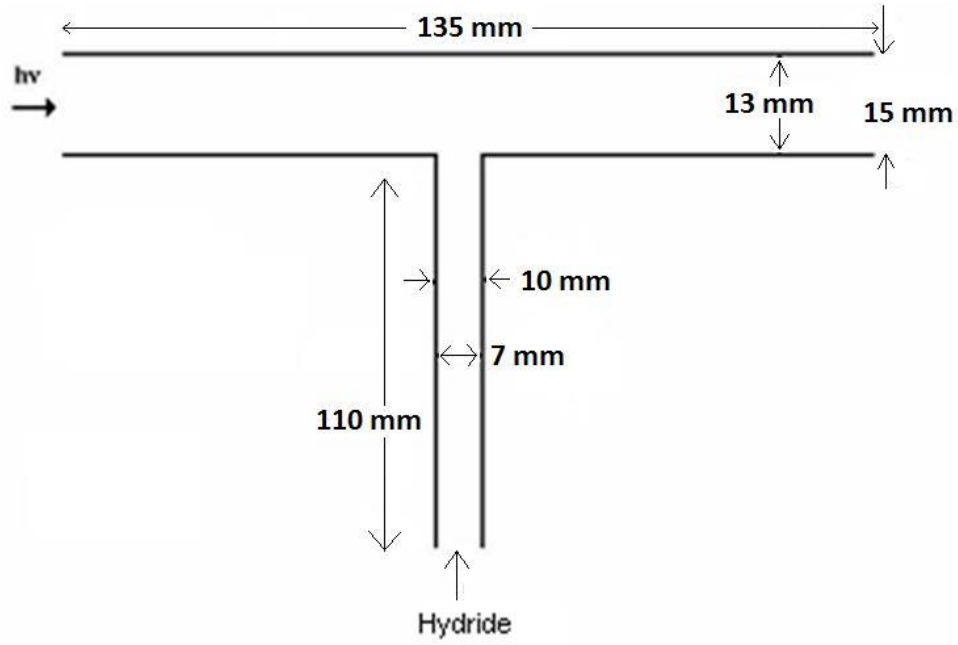

Figure 11 Schematic representation of externally heated quartz tube atomizer.

2.3.1 Continuous Flow Vapor Generation System

PTFE connection tubing (Cole Palmer) with 0.56 mm i.d. were used for the reaction coil in the continuous system.Schematic representation of the continuous flow vapor generation system is illustrated in Figure 12.

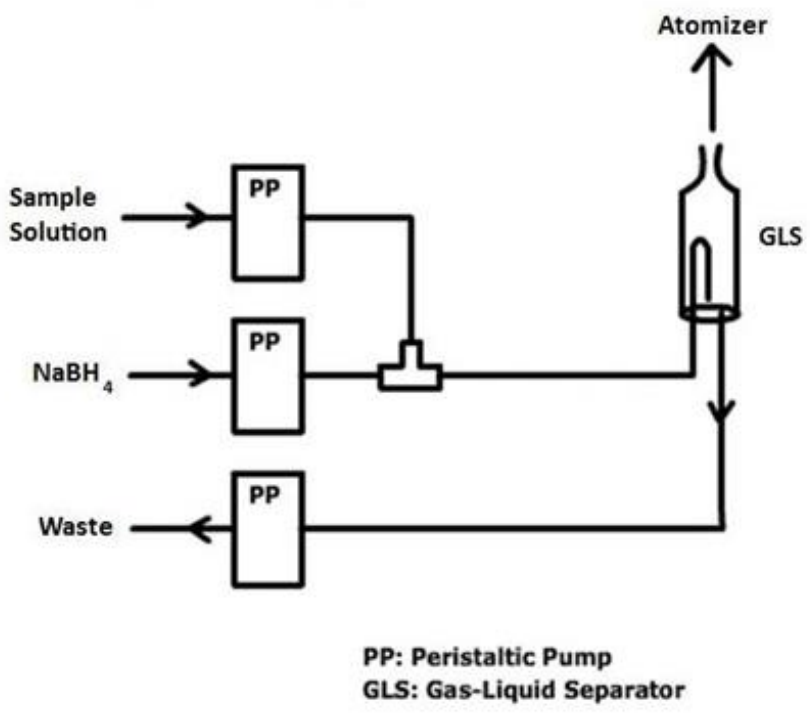

Figure 12: Schematic representation of the continuous flow vapor generation system

In order to separate the volatile product from the liquid phase, a laboratory made borosilicate GLS was used right after the stripping coil. Separated volatile species were transferred to the atomizer by the help of a PTFE tubing with 0.4 mm inner diameter. Dimensions and schematic diagrams of the GLS used is given in Figure 13.

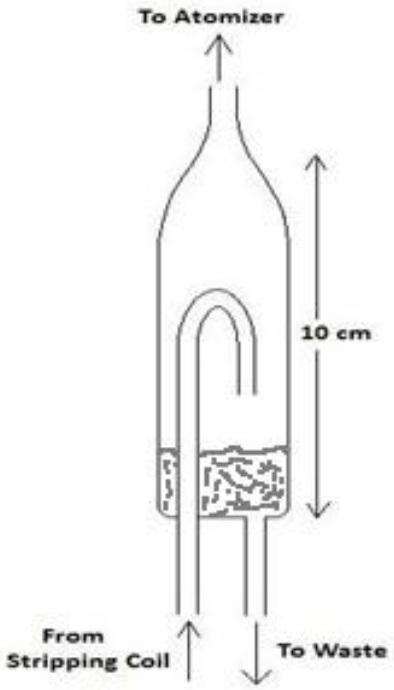

Figure 13 Schematic representation of GLS used in continuous flow system.

2.3.2 Flow Injection Vapor Generation System

A 6-way injection valve was used in order to introduce the analyte into the flow injection system.

A 4 way PTFE connector (Cole Palmer, Illinois, USA) was used in order to mix the reducing $NaBH_4$ solution, carrier HCl solution and analyte, and carrier high purity Ar. Mixing of the solutions occurred at the center of the PTFE connector. Schematic representation of the system is given in Figure 14.

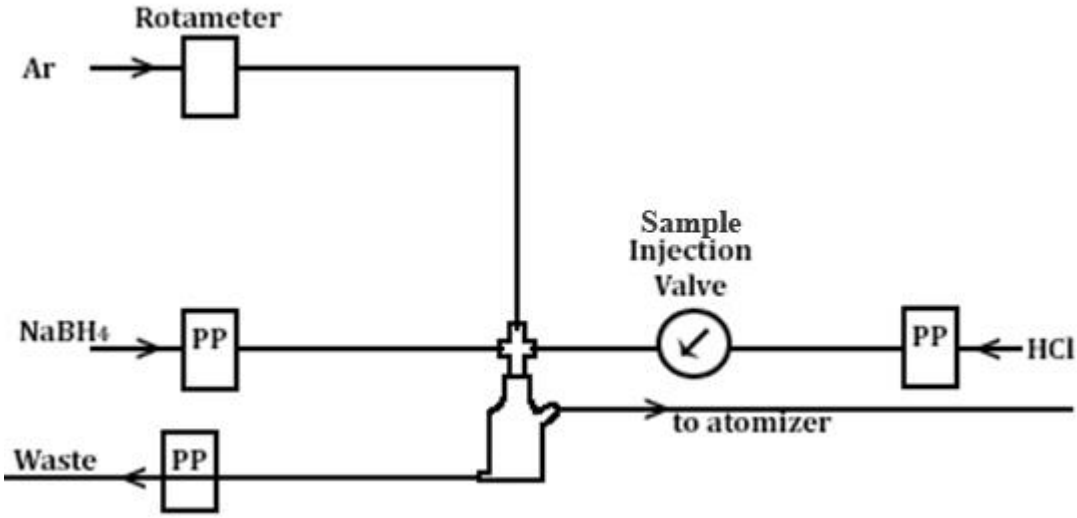

Figure 14 Schematic representation of the flow injection vapor generation system.

Different from the traditional VG systems, there was no reaction and stripping coil in the flow injection VG system in this study. Solutions and carrier Ar were mixed in the center of the 4-way PTFE connector and moved to the GLS concurrently. To help transportation of the volatile species through the atomizer, a cylindirical GLS with 3.0 mL volume, 56 mm height and 12 mm outer diameter was prepared.

During flow injection studies, a quartz capillary tube was placed inside the inlet arm of the QTA to introduce high purity oxygen into the system. Quartz capillary tube with approximately 0.5 mm outer diameter was prepared by using a quartz tube with 4.0 mm outer and 3.0 mm inner diameter. Positioning of the tube is represented in Figure 15. This collection system was used by Dedina and his collaborators (Kratzer & Dedina, 2008). For investigation of nature of the volatile species, 0.2 μm pore sized syringe filters (Pall) were used.

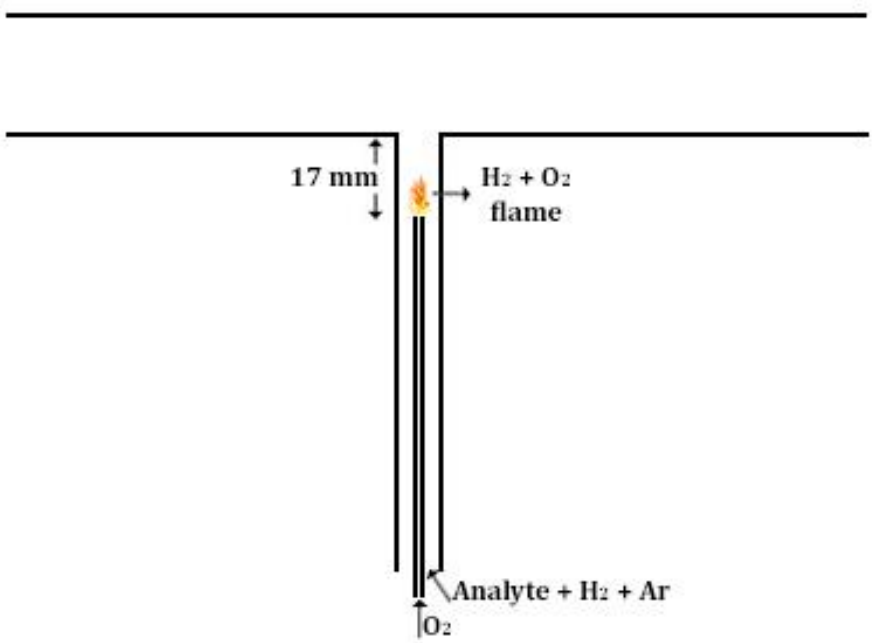

Figure 15: Schematic representation for introduction of oxygen in quartz atom trap

2.3.3 UV Photochemical Vapor Generation

A simple UV reactor was prepared, which was devised by Sturgeon and his coworkers (Xuming et al., 2013), using a 6 W, 254 nm Hg lamp in order to achieve reduction of In prepared in various low molecular weight organic acids such as formic acid, acetic acid and propionic acid. Indium solutions were passed through PTFE tubing with 0.8 mm diameter and 5 m length wrapped around the Hg lamp with 6W power and 254 nm wavelength. An external hydrogen source was used to introduce 15.0 mL/min H_2 and an external Argon source was used to introduce 55.0 mL/min Ar into the system. System is illustrated in Figure 16.

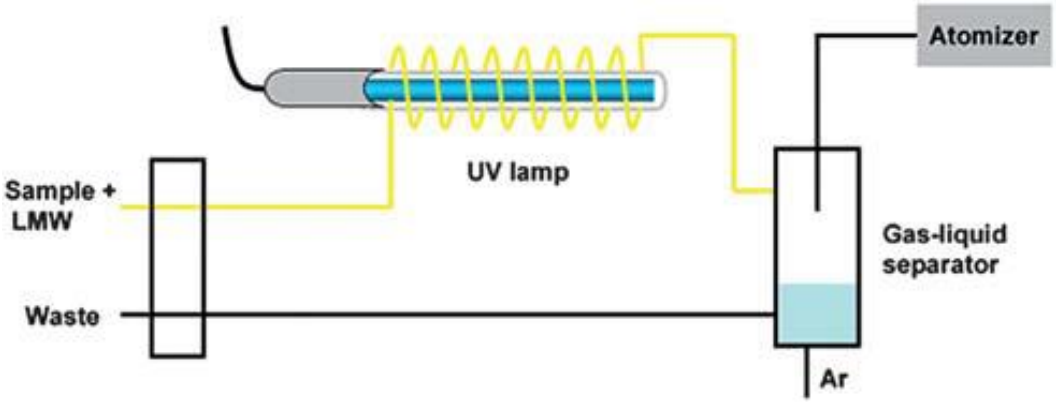

Figure 16: Schematic representation of a UV photochemical vapor generation system (Xuming et al., 2013).

2.4 Procedures

2.4.1 Continuous Flow Vapor Generation

For the continuous flow vapor generation system, analyte indium solutions were acidified with HCl to get the final solution in 2.0 to 3.0 mol/L HCl. Solution flow rate was optimized and used as 8.0 mL/min. Reductant solution of $NaBH_4$ was optimized and used as 6.0 % (w/v). Reductant solution was prepared in 0.6% (w/v) of NaOH. Flow rate for $NaBH_4$ was optimized to 12.0 mL/min. Flow rate of argon for stripping the volatile species was optimized to 0 mL/min. Volatile species formed were transported to the atomizer by the help of the hydrogen that is formed in the HCl-$NaBH_4$ reaction. Reaction coil length was optimized to 12.0 cm. Integrated signal was collected for 10 seconds and result is calculated as the mean of three replicate measurements.

2.4.2 Flow Injection Vapor Generation

For the flow injection VG studies, Carrier HCl concentration and flow rate were optimized and used as 0.47 mol/L and 3.0 mL/min, respectively. Reductant $NaBH_4$ concentration and flow rate were optimized to 3.0% (w/v) and 3.0 mL/min. Concentration of the NaOH for stabilization of $NaBH_4$ was set to 0.3% (w/v). Loop sizes varying in the range of 500 to 2000 µL were used; standard In solutions contained 0.47 mol/L HCl. Mixing of the solutions and carrier argon took place at the center of the 4-way PTFE connector. Volatile species generated were carried through the GLS by the help of argon supply with 300.0 mL/min flow rate and hydrogen that was produced from the HCl-$NaBH_4$ reaction. Blank solutions are used as 0.47 mol/L HCl.

In order to trap the volatile indium species on the surface of the quartz tube atomizer, an external oxygen source was used. Oxygen was introduced inside the inlet arm of the QTA with 80.0 mL/min flow rate using a quartz capillary tube. A hydrogen-oxygen flame was formed on the end of the capillary with the hydrogen that was produced from the HCl-$NaBH_4$ reaction and the oxygen gas that was supplied externally.

Duration for oxygen introduction, i.e. collection time, was optimized to 60 seconds. A stopwatch was used to arrange the timing. Stopwatch is started when oxygen is introduced to the system. At the 5^{th} second, analyte indium solution was injected into the carrier HCl solution. Oxygen flow was stopped at 65^{th} second and signal was formed right after the hydrogen-oxygen flame disappears inside the inlet arm of the quartz T-tube atomizer.

Further discussion on the quartz trap is made in the Results and Discussion part.

2.4.3 UV Photochemical Vapor Generation

For photochemical generation of indium volatile species, sample solution was transported to the system with 3.0 mL/min flow rate for 1.5 minutes. Then pumps were turned off in order to make sample solution exposed to UV radiation for 3 minutes. After 3 minutes, pumps were turned on in order to send de-ionized water into the UV reactor, so that solution containing analyte will be directed to GLS. In order to help transportation of volatile species through the atomizer, Ar and hydrogen were introduced at the end of GLS with 55.0 and 15.0 mL/min flow rates, respectively.

CHAPTER 3

RESULTS AND DISCUSSION

This study involves development of an alternative sensitive analytical method for determination of indium with low detection limits.

In the first part, determination of indium by conventional continuous flow VGAAS system was studied. Flow rates of $NaBH_4$, carrier HCl solution and carrier Ar gas and concentrations of $NaBH_4$ and HCl were optimized. In this part of the study, reproducibility of the signals were affected by the high memory problem and fast decomposition of volatile species generated. These made further development of the method impracticable and linear range and calibration studies could not be achieved.

Second part consisted of determination of indium by flow injection VGAAS and trapping on the surface of the quartz T-tube atomizer. In this design, broadening of the peak was minimized and satisfying signals were achieved in order to continue on linear range and calibration studies.

In the third part of this study, sources of memory effect were investigated in the FI-VGAAS system. After saturation of the system with 10.0 mg/L indium standard solution, different parts of the system were replaced with the new one and flow injection VGAAS signal of blank solution were observed.

In the fourth part of this study, vapor generation efficiency of indium was investigated. Waste solutions collected from the GLS were analyzed using ETAAS.

In the fifth part, nature of the volatile indium species was investigated. Volatile species were passed through a 0.2 μm pore size filter in order to check whether they

are in molecular form or not. Also, volatile species were collected on the surface of quartz plates and analyzed using a Raman spectrometer.

In the last part of the study, an alternative vapor generation system was tested. In this system, indium standard solutions in various organic acids were subjected to UV radiation in order to investigate whether any volatile species form or not. Due to insufficient efficiency of vapor generation of indium by UV irradiation, this part was failed.

3.1 Continuous Flow Vapor Generation System

Volatile species are generated in continuous mode in this part. Optimization studies are described in the following parts.

3.1.1 Optimization of $NaBH_4$ and Sample Solution Flow Rates

In this part of the study, 10.0 mg/L indium standard solution was prepared in 3.0 mol/L HCl. Reducing reagent was initially 4.0% (w/v) $NaBH_4$. Carrier gas was not used throughout the experiment. Volatile indium species are transported with hydrogen generated in the $NaBH_4$ – HCl reaction. HCl flow rate was kept constant at 8.0 mL/min and $NaBH_4$ flow rate was varied between 4.0 and 20.0 mL/min. Optimum value for reducing reagent flow rate was chosen as 12.0 mL/min in which absorbance value read from the instrument was 3 times better compared to that of 4.0 mL/min flow rate. Results are show in Figure 17.

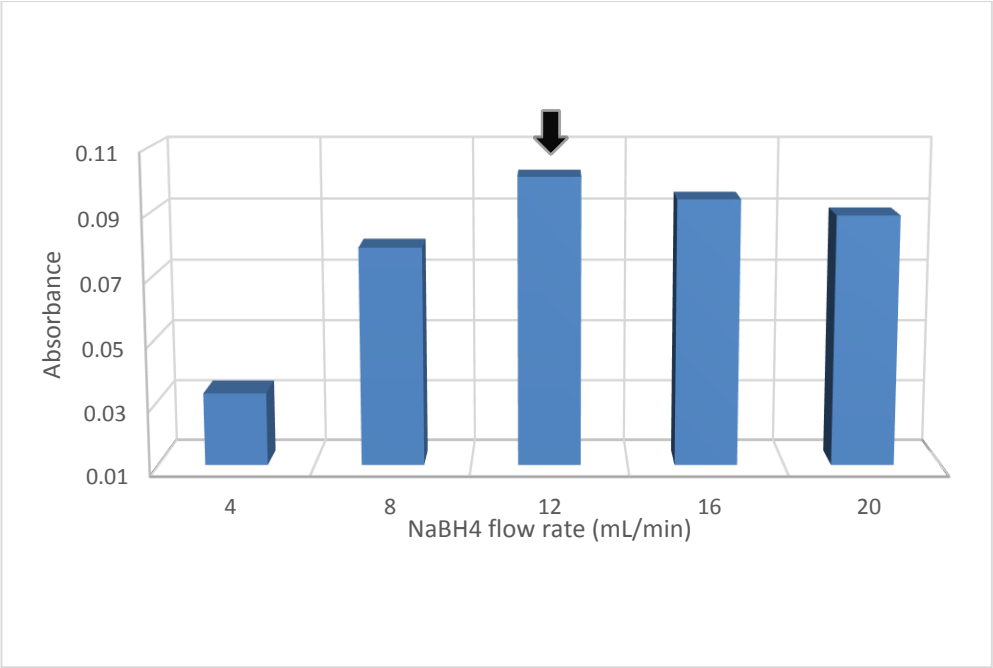

Figure 17 Effect of $NaBH_4$ flow rate on the continuous flow VGAAS signal of 10.0 mg/L In solution prepared in 3.0 mol/L HCl.
Sample was sent with the flow rate of 8.0 mL/min and carrier Ar was not used. $NaBH_4$ concentration was set as 4.0% (w/v). NaOH concentration was 0.4% (w/v).

Once $NaBH_4$ flow rate was optimized, effect of sample solution flow rate was optimized. In this part, flow rate of the sample solution which is prepared in 3.0 mol/L HCl was varied between 4.0 mL/min to 20.0 mL/min. $NaBH_4$ solution flow rate was kept constant at 12.0 mL/min during this study. 8.0 mL/min was selected as optimum. Results are shown in Figure 18.

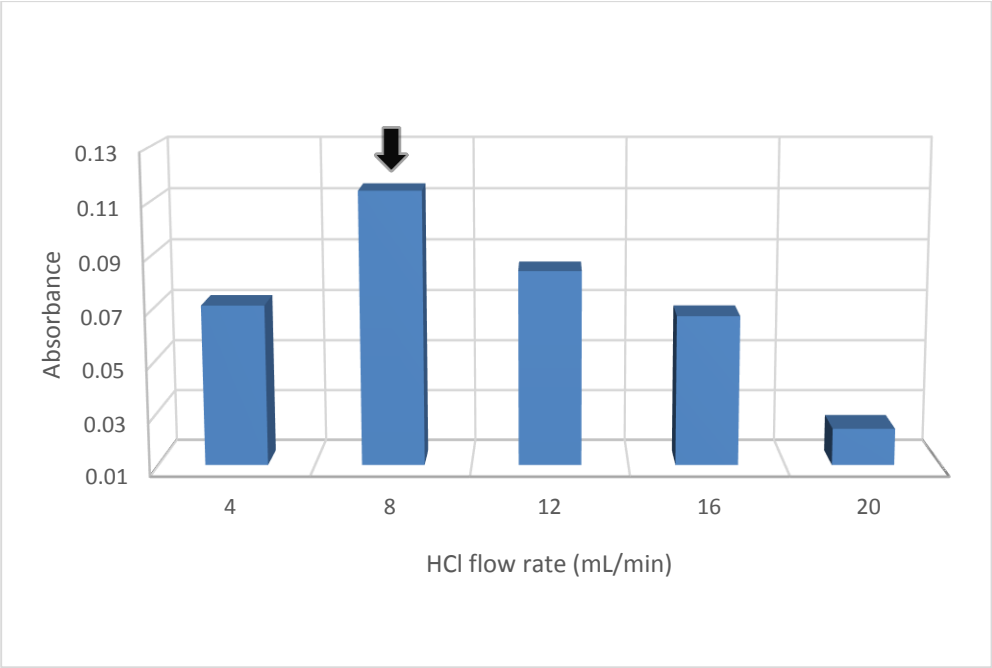

Figure 18 Effect of sample flow rate on the continuous flow VGAAS signal of 10.0 mg/L In solution prepared in 3.0 mol/L HCl.
4.0% (w/v) $NaBH_4$ prepared in 0.4% /w/v) NaOH was used with a flow rate of 12.0 mL/min. Carrier gas was not used throughout this study.

3.1.2 Optimization of Ar Flow Rate

Ar was used in order to transport volatile species to the atomizer. Carrier gas affects concentration and residence time of volatile species in the measurement zone. Effect of Ar flow rate to the analytical signal was examined with different flow rates of Ar from 0 to 200 mL/min. As a result of this study, absorbance values tend to decrease with increasing flow rate. This was an expected result. As discussed above, higher flow rates of carrier Ar results in dilution of the volatile species in the optical path. In addition, if volatile species are transported with a higher flow rate, then residence time of those will be less. As it is summarized in Figure 19, the highest absorbance was obtained in the absence of carrier Ar.

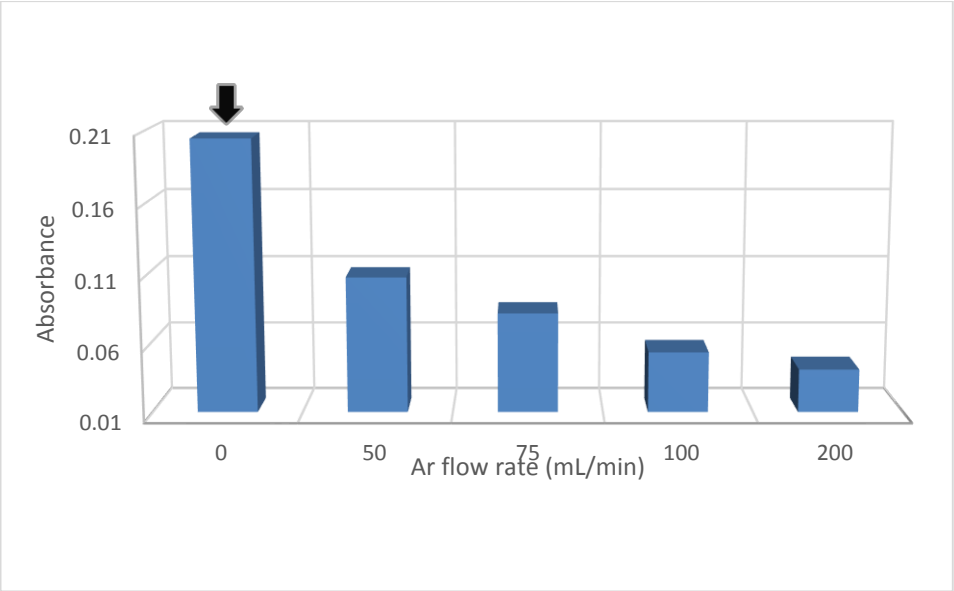

Figure 19 Effect of Ar flow rate on the continuous flow VGAAS signal of 10.0 mg/L In solution prepared in 3.0 mol/L HCl.
Sample flow rate was 8.0 mL/min. 4.0% (m/v) $NaBH_4$ was used with a flow rate of 12.0 mL/min.

3.1.3 Optimization of HCl and $NaBH_4$ Concentration

Reductant and acid concentrations are important in VG systems since ratio between these two determines the pH of the reaction medium and also the amount of hydrogen produced in order to transport and facilitate the atomization of volatile species in the measurement zone. Since their interaction is important, optimization of these two parameters was carried out together. All $NaBH_4$ solutions were prepared in 0.5% (w/v) NaOH in order to prevent hydrolysis. Results showed that 6.0% was optimum for $NaBH_4$ concentration and 2.0 mol/L was optimum for HCl concentration. Higher concentrations of reducing reagent results in higher amount of hydrogen which is used to transport and also facilitate the atomization of the volatile species generated. HCl concentration of 2.0 mol/L can be explained by means of optimum pH of the reaction medium.

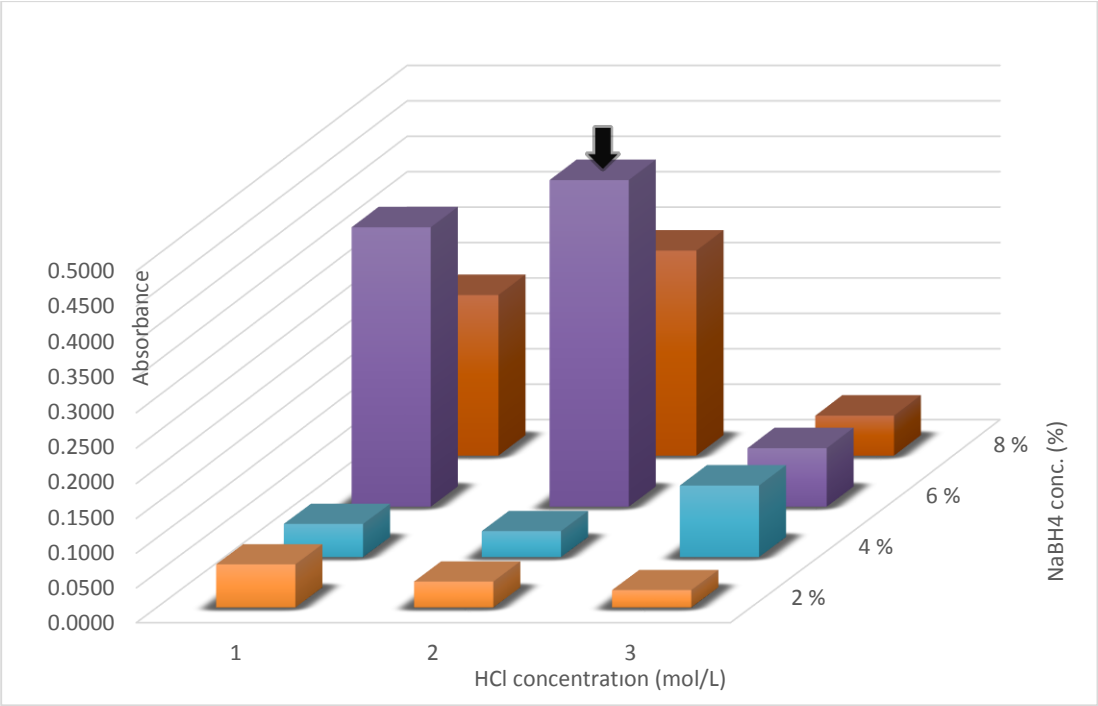

Figure 20 Effect of HCl and $NaBH_4$ concentration on the CF-VGAAS signal of 10.0 mg/L In solution prepared in 3.0 mol/L HCl.

Experiments were conducted in the absence of a carrier gas. $NaBH_4$ solutions were prepared in 0.5% NaOH. Sample and $NaBH_4$ flow rates were set as 8.0 mL/min and 12.0 mL/min, respectively.

3.1.4 Results of Continuous Flow VG System

Further optimizations and calibration studies for conventional continuous flow VG system were not held due to unstable reaction and atomizer conditions and also high memory effect in the system. Also as a result of high $NaBH_4$ concentrations, devitrification on the quartz tube atomizer lowered the sensitivity of the system frequently. These deficiencies resulted in low reproducibility in the system with % RSD values ranging from 10-40. Parameters that are optimized for Continuous Flow VGAAS system are summarized in Table 7. GLS in this system was changed with a

smaller one and reaction coil was removed for further studies in order to compensate the problemes due to decomposition of the volatile species. Moreover, for better sensitivity, the system was coupled with quartz trap.

Table 7 Optimized parameters for continuous flow vapor generation system.

Parameter	**Optimum Value**
$NaBH_4$ flow rate	12.0 mL/min
Sample flow rate	8.0 mL/min
Ar flow rate	-
$NaBH_4$ concentration	6.0% (w/v)
HCl concentration	2.0 mol/L

3.2 Flow Injection Vapor Generation System with Quartz Trap

In this part of the study, In volatile species are generated in flow injection mode, GLS was changed with smaller one, reaction coil was removed and then parameters were optimized to increase sensitivity.

3.2.1 Optimization of Ar Flow Rate

2.0 mg/L In solution was used as analyte. Carrier HCl concentration was selected as 0.40 mol/L and analyte solution was acidified with HCl to get a final concentration of 0.40 mol/L. Sample was introduced into the system via injection valve using a 500 µL loop. 2.0% (w/v) $NaBH_4$ stabilized in 0.2% (w/v) NaOH was used as reductant solution. Carrier HCl and reductant $NaBH_4$ was introduced into the system with 3.0 mL/min flow rate. At the beginning, oxygen was introduced into the system for 40 seconds with 80 mL/min flow rate. Position of the capillary tube used for oxygen introduction was 1.0 cm from the junction point of optical arm and inlet arm. Temperature of the electrical furnace used to heat the QTA was set to 1030 °C. Argon flow rate was varied from 50 to 300 mL/min. Signal height was observed to increase with increasing Ar flow rate. At lower flow rates of Ar, signal shapes were broad and heights were lower because of low transportation efficiency. Moreover, when transportation is slower, volatile species tend to be either adsorbed on the wet surface of the GLS and the tubing; or decompose before reaching to the optical arm. On the other hand, when argon flow rate is at higher levels, signal heights decreased, most probably due to dilution of the volatile species in the optical arm of the QTA and shorter residence time in the atomizer due to high flow rates. Thus, optimum value for Ar flow rate was chosen as 300 mL/min. A summary of the results are shown in Figure 21.

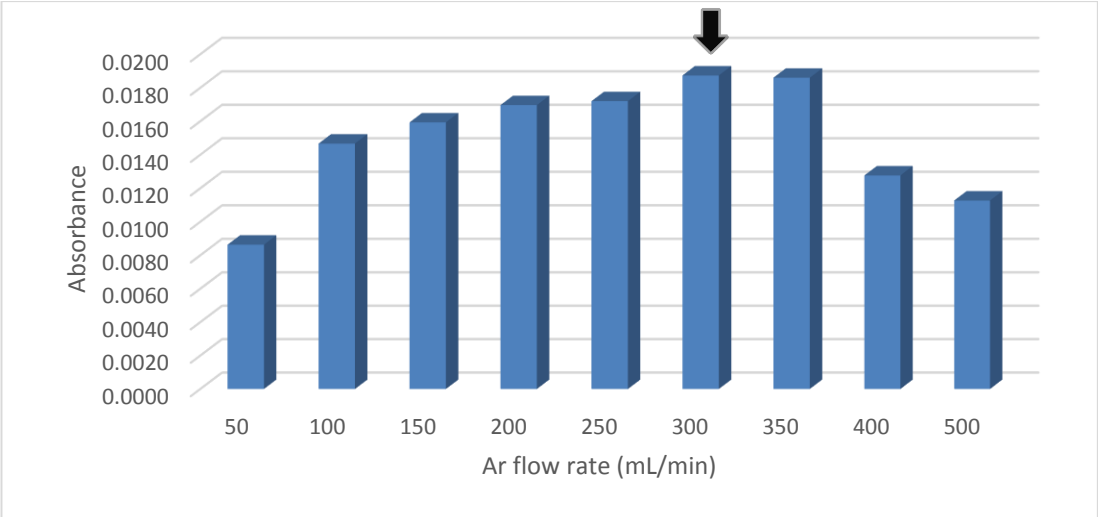

Figure 21 Effect of Ar flow rate on the flow injection VGAAS signal of 2.0 mg/L In. 0.40 M HCl as carrier, 2.0% $NaBH_4$ in 0.2% NaOH as reductant solutions, with 3.0 mL/min flow rates for both. Oxygen was introduced for 40 seconds with 80 mL/min flow rate. Loop volume was chosen as 500 µL.

3.2.2 Optimization of O_2 Flow Rate

Efficiency of the quartz trap depends strongly on the volume of oxygen introduced into the system. In order to trap all the volatile species of indium on the surface of the quartz T-tube atomizer, all the hydrogen that is produced in the HCl-$NaBH_4$ reaction must react with sufficient oxygen and no hydrogen should present in the optical arm. When there is no hydrogen in the optical arm, indium volatile species are adsorbed or decomposed on the QTA surface, being ready to be atomized when hydrogen is reached to the optical arm. When hydrogen reaches to the optical arm of the QTA, it constitutes a convenient atmosphere for the atomization of indium. The mechanism of hydrogen assistance to the atomization is not exactly known. This fact is illustrated in Figure 22.

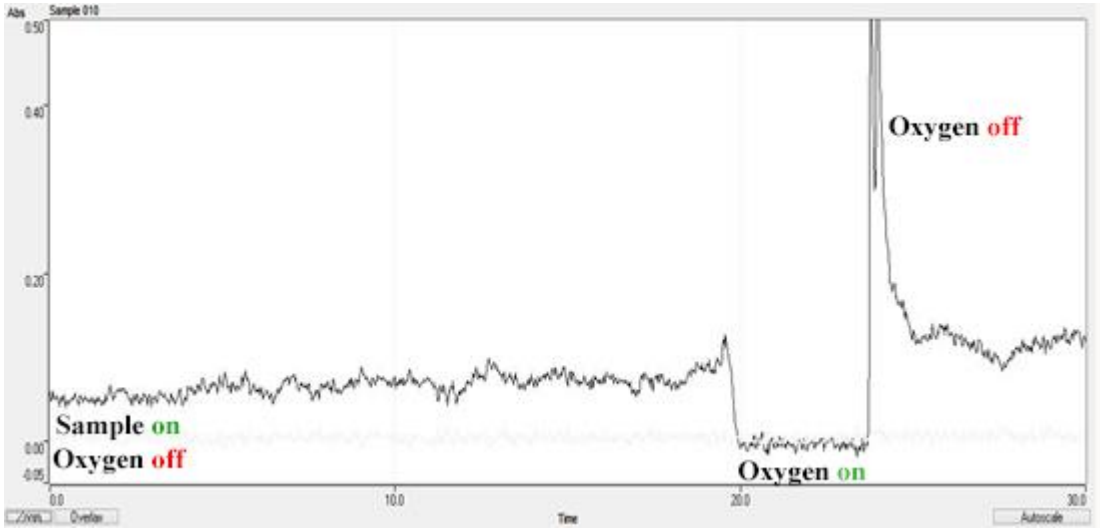

Figure 22: Continuous flow signal decreases with increasing oxygen flow.

In this part of the study, 2.0 mg/L solution was used as analyte. Carrier solution and analyte solution were acidified with 0.40 mol/L HCl. Sample loop volume for analyte injection was 500 µL. $NaBH_4$ concentration and flow rates of $NaBH_4$ and carrier were 2.0 % (w/v) and 3.0 mL/min, respectively. Ar flow rate was set to 300 mL/min. Oxygen was introduced into the system for 40 seconds and flow rate was altered between 30 and 100 mL/min. At lower flow rates, signal heights were lower since some of the indium volatile species were atomized with the help of remaining hydrogen gas reached to the optical arm. When oxygen flow rate increased, all the hydrogen was reacted inside the inlet arm of the QTA and consumed, so atomization of volatile indium species was not favored in the optical arm. At higher flow rates, no difference in the signal heights was observed. Optimum value for O_2 flow rate was chosen as 80 mL/min. Results are summarized in Figure 23.

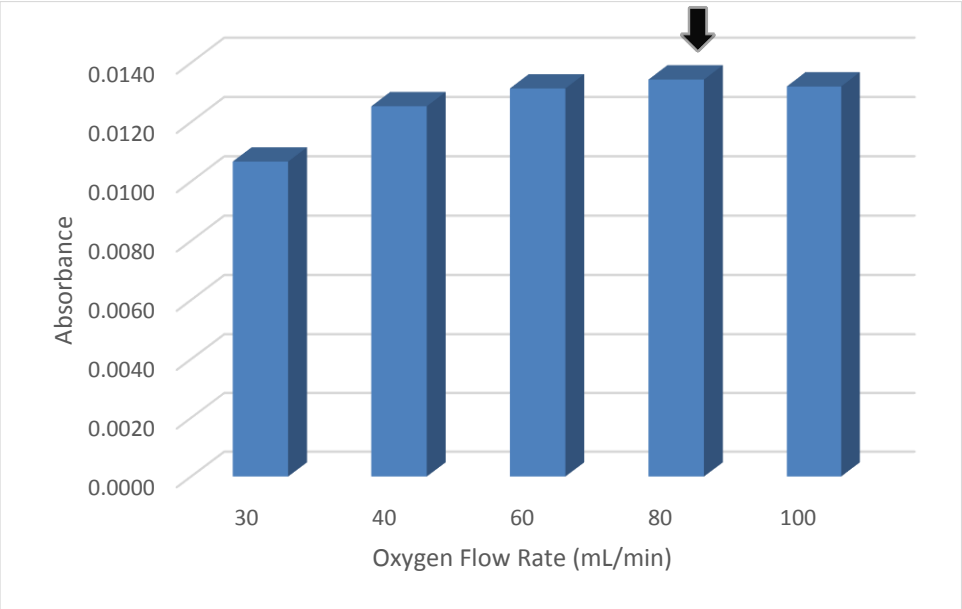

Figure 23 Effect of O_2 flow rate on the flow injection VGAAS signal of 2.0 mg/L In. 0.40 M HCl as carrier, 2.0% (w/v) $NaBH_4$ in 0.2% (w/v) NaOH as reductant solutions were used, with 3.0 mL/min flow rates for both. Oxygen was introduced for 40 seconds. Loop volume was chosen as 500 µL.

In order to choose the best flow rate for oxygen, hydrogen that is produced per minute was measured experimentally. For this purpose, a simple set-up was prepared using a sealed Schlenk flask, connected to a graduated glass tube with silicon tubing. Glass tube was filled with water. 1.0 mL of 3.0% (w/v) $NaBH_4$ was placed in the Schlenk tube, sealed and connected to the glass tube. When 1.0 mL of 0.47 mol/L HCl was injected into the tube, 54 mL of water was removed from the system after the reaction is completed. This procedure was repeated three times and same result was observed. Thus, with 3.0 mL/min flow rate of HCl and $NaBH_4$, a 162 mL of hydrogen is produced per minute in the system. Considering this result and the experimental optimization result discussed above, external oxygen flow rate was chosen as 80 mL/min to finish all of the produced hydrogen in the system.

3.2.3 Optimization of Collection Time

Collection time, i.e. the time interval in which oxygen was introduced into the system is important. It should be long enough that all of the produced volatile species should reach to the atomizer from the GLS.

In this part, argon and oxygen flow rates were set to 300 and 80 mL/min, respectively. Collection time was varied between 30 and 80 s and optimum collection time was selected as 60 seconds. Longer collection times did not change the analytical signal. If oxygen was introduced for shorter times, signal heights were shorter and signals were broader as expected since all the volatile species were not collected. Results of the collection time optimization are illustrated in Figure 24.

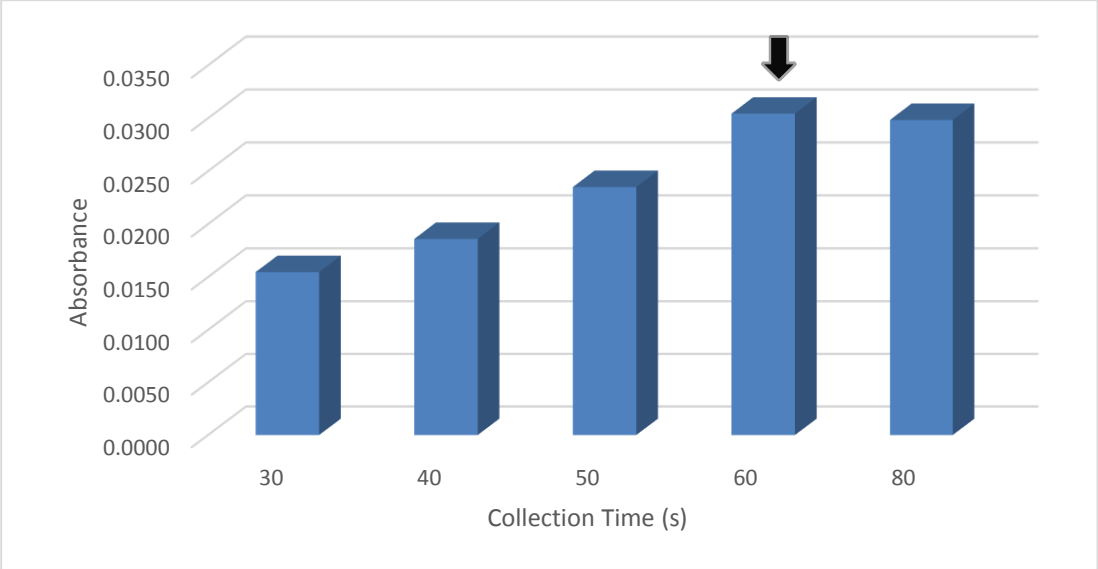

Figure 24: Effect of collection time on the signal of 2.0 mg/L In solution.
Flow rate of carrier liquid and $NaBH_4$ were set as 3.0 mL/min. HCl and $NaBH_4$ concentrations were 0.40 mol/L and 2.0% (w/v) respectively. 500 µL loop volume was used and Ar flow rate was set to 300 mL/min. Oxygen flow rate was 80 mL/min.

3.2.4 Sample Loop Volume Optimization

Injection of indium standard solution into the carrier HCl was achieved by the help of a 6-way sample injection valve. 500, 1000 and 2000 µL loops were examined in this part of the study. Signal heights were increased with increasing loop volumes since the amount of volatile species reaching to the quartz tube atomizer was increasing with increasing loop volume. On the other hand, signals get broader and time needed to complete one single analysis increase with increasing loop volume. For this reason, 2.0 mL sample loop was not chosen. Optimum loop volume was selected to be 1000 µL. Results are illustrated in Figure 25.

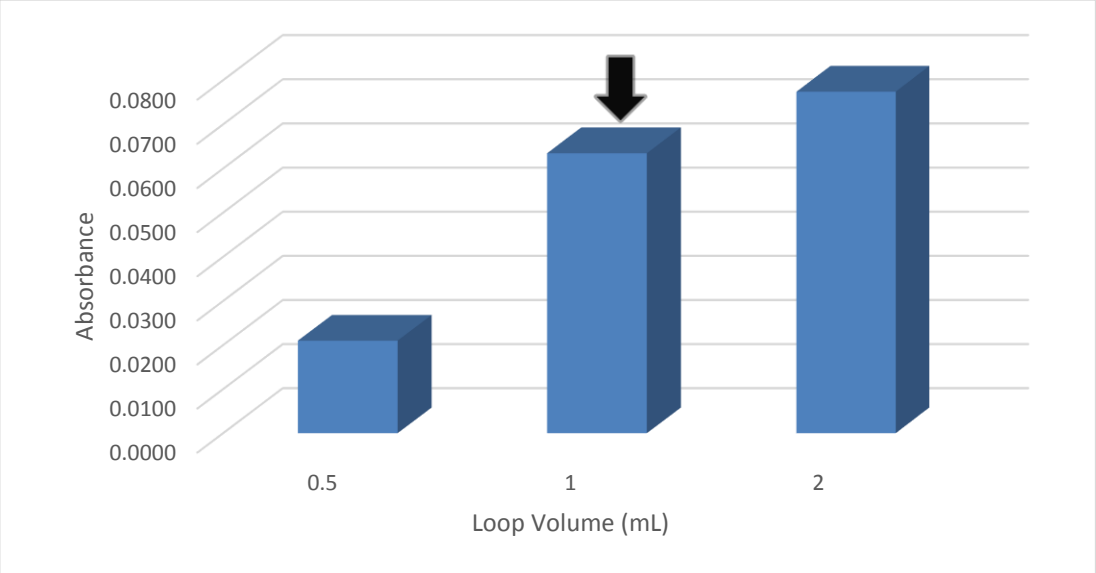

Figure 25: Effect of sample loop volume on the flow injection VGAAS signal of 1.0 mg/L In solution prepared in 0.47 mol/L HCl.

Argon flow rate was set to 300 mL/min. Oxygen was sent to the atomizer for 60 seconds with 80 mL/min flow rate. HCl and $NaBH_4$ flow rate was 3.0 mL/min and concentrations were 0.47 mol/L and 3.0 %, respectively.

3.2.5 Optimization of $NaBH_4$ and HCl Concentrations

Reductant and acid concentrations strongly affect the VG reaction. Because amount of hydrogen produced affects the atomization of indium. Moreover, pH of the reaction medium, which affects efficiency of generation of volatile species changes with different concentrations of HCl and $NaBH_4$. To find out the optimum concentrations of carrier acid and reductant solution, 2.0 mg/L indium standard solution was used as the analyte. Sample loop volume was chosen as 500 µL and oxygen was introduced into the system for 40 seconds with a flow rate of 80 mL/min. Ar flow rate was 300 mL/min. HCl concentration was varied from 0.2 to 0.8 mol/L and $NaBH_4$ concentration was varied from 1.0 to 4.0% (w/v). As summarized in Figure 26, 0.40 mol/L was chosen as the optimum concentration for carrier HCl and 3.0% for reductant.

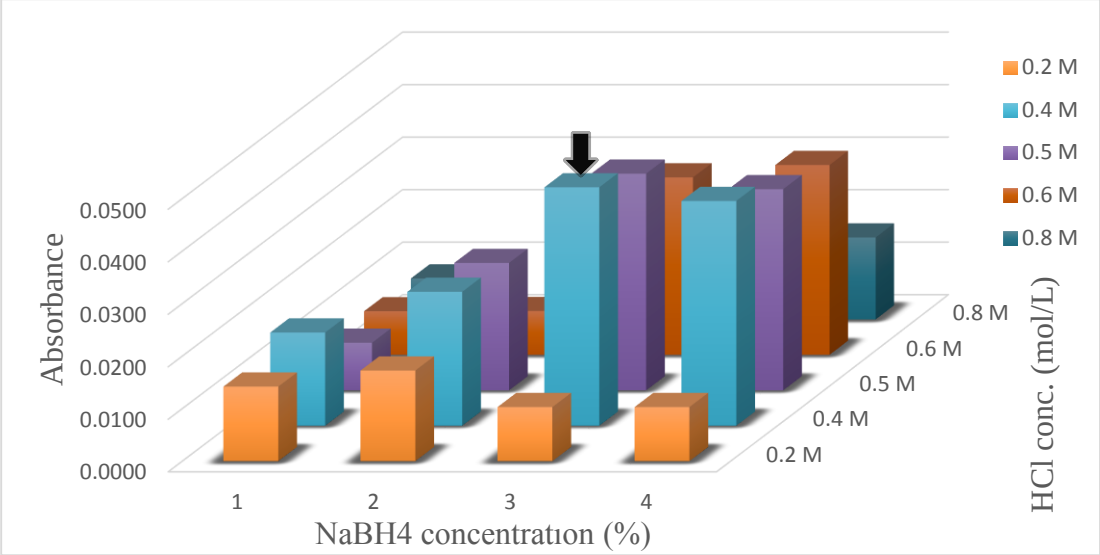

Figure 26 Effect of $NaBH_4$ and HCl concentrations on the flow injection VGAAS signal of 2.0 mg/L In solution.

Flow rate of carrier liquid and $NaBH_4$ were set as 3.0 mL/min. 500 µL loop volume was used and Ar flow rate was set to 300 mL/min. Oxygen flow rate was 80 mL/min with 40 s introduction time.

Using a 2-factor 4-level factorial experimental design, optimum acid and reductant concentrations were calculated with the experimental data. Optimum concentrations of HCl and $NaBH_4$ were found out to be 0.47 mol/L and 3.0% respectively. Results are illustrated in Figure 27.

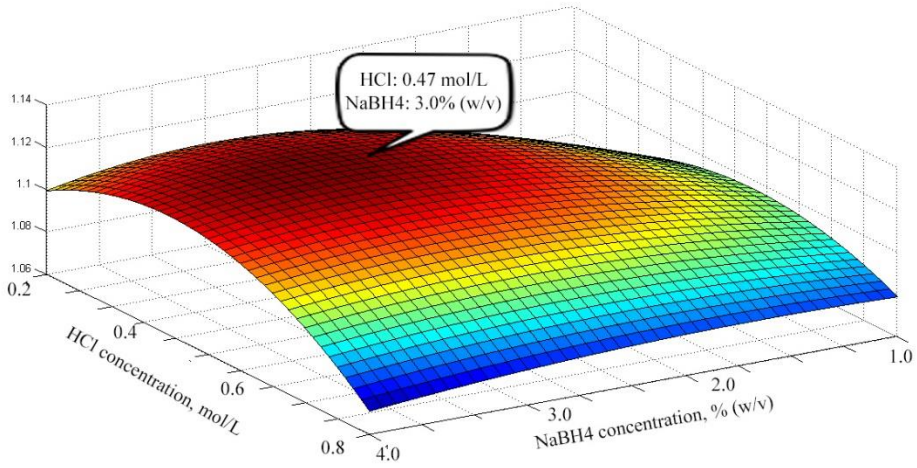

Figure 27: 2 factor 4 level factorial 3D experimental design plot for effect of $NaBH_4$ and HCl concentrations on the flow injection VGAAS signal of 2.0 mg/L In solution.

3.2.6 Optimization of $NaBH_4$ and HCl Flow Rates

Reductant $NaBH_4$ and carrier HCl flow rates were varied between 1.0 and 4.0 mL/min using a peristaltic pump. As expected, signal heights of 1.0 mg/L indium standard solutions increased with increasing flow rates of $NaBH_4$ and HCl. However, 4.0 mL/min flow rate was not chosen due to the difficulty faced in management of flow rate in small volume of GLS. When a larger GLS was used instead of the small one, signals were broader, so 3.0 mL/min flow rate of $NaBH_4$ and HCl was chosen using the smaller GLS. Results of HCl and $NaBH_4$ flow rates are shown in Figure 28.

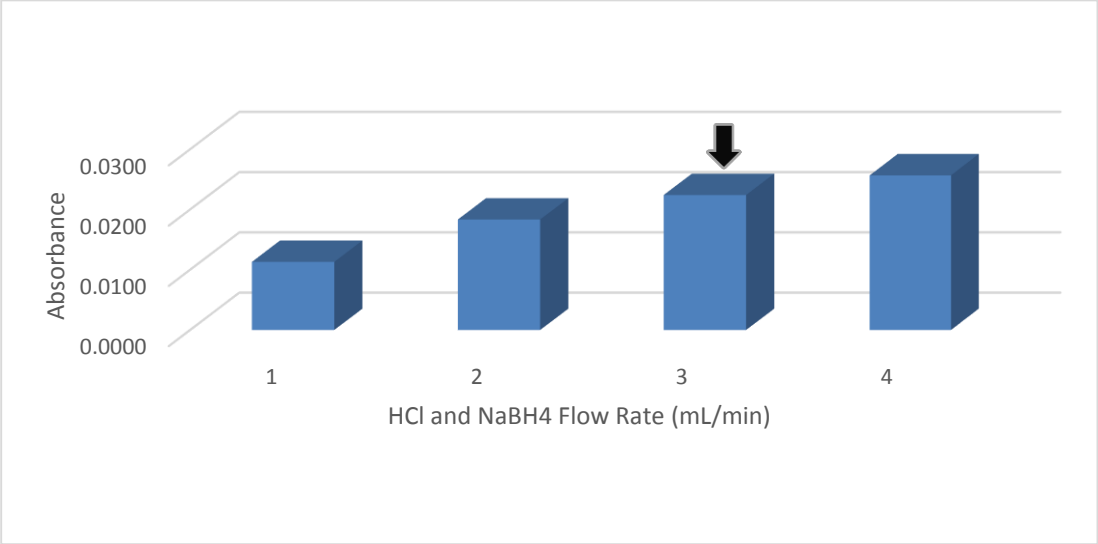

Figure 28 Effect of $NaBH_4$ and carrier liquid flow rates on the flow injection VGAAS signal of 1.0 mg/L In solution prepared in 0.47 mol/L HCl.
3.0% (m/v) $NaBH_4$ was used. 500 µL loop volume was used for sample introduction. Ar and O_2 flow rates were set to 300 and 80 mL/min, respectively. Volatile species were collected for 60 s.

3.2.7 Effect of Hydrogen Introduction

Hydrogen plays an important role for the atomization of volatile species inside the quartz T-tube atomizer. When the volatile species of indium are generated chemically, hydrogen is produced from the reaction between HCl in the carrier solution and reductant $NaBH_4$. Amount of produced hydrogen can be changed by changing HCl and $NaBH_4$ concentrations. However, pH of the reaction medium also changes, which also affects the volatile species generation. Thus, for further investigation of the effect of hydrogen concentration in the measurement zone, hydrogen gas was introduced into the system externally.

In order not to affect the reaction medium, hydrogen was introduced to the atomizer after the GLS. Time for introduction was five seconds after stopping oxygen introduction. Flow rate of hydrogen was varied between 0 and 110 mL/min. Neither signal heights nor signal shapes were changed with different hydrogen flow rates. Thus, it was decided external hydrogen was not to be necessary for the system, as shown in Figure 29.

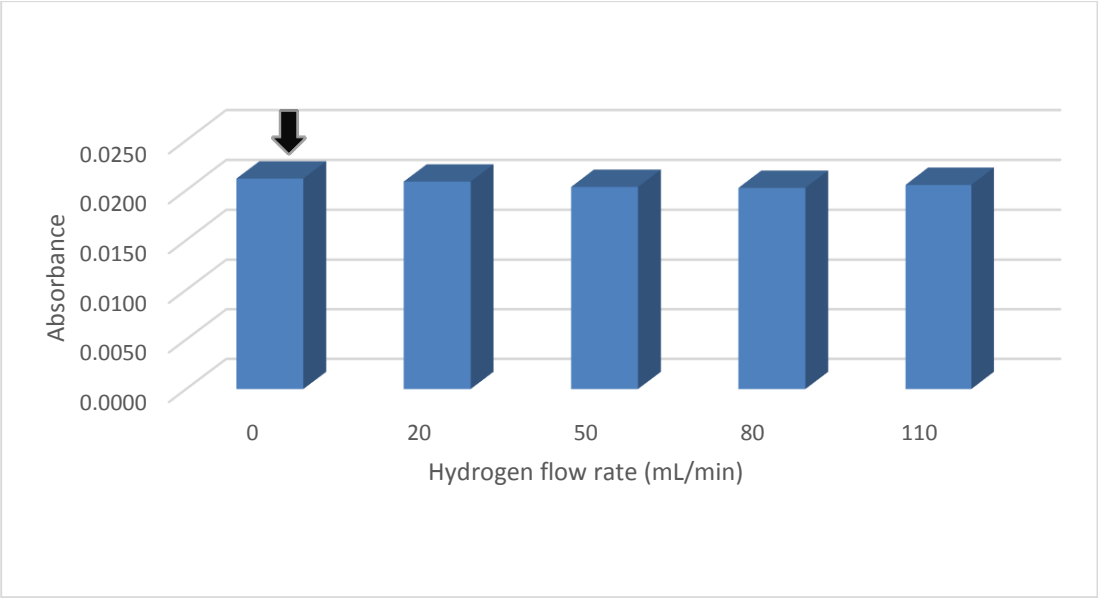

Figure 29 Effect of H_2 introduction through the atomizer to the VGAAS signal of 1.0 mg/L indium standard solution prepared in 0.47 mol/L HCl.
Carrier and reductant flow rate was 3.0 mL/min with concentrations 0.47 mol/L and 3.0% respectively. Oxygen was introduced for 60 s with 80 mL/min flow rate. Argon flow rate was set as 300 mL/min.

3.2.8 Optimization of NaOH Concentration

In this study, reductant $NaBH_4$ solution was prepared daily. In order to decrease the rate of hydrolysis of the reductant solution, NaOH was also used as stabilizer. Concentration of NaOH can be important since it affects the pH of reaction medium. To observe the effect of NaOH concentration on the analytical signal, reductant solution was prepared with different NaOH concentrations between 0.10 and 0.50% (w/v). No significant change in the signal heights was observed between 0.10 and 0.30% and slight difference was observed between 0.30 and 0.50%. 0.30% was chosen as NaOH as illustrated in Figure 30.

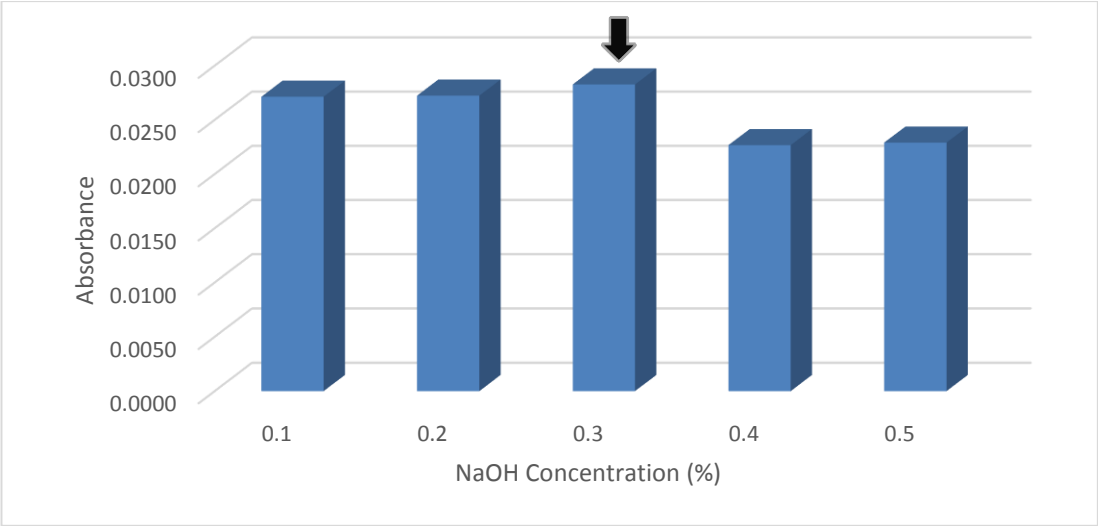

Figure 30 Effect of NaOH concentration on the flow injection VGAAS signal of 1.0 mg/L In solution prepared in 0.47 mol/L HCl.

Argon and oxygen flow rates were 300 and 80 mL/min, respectively. Carrier and reductant concentrations were 0.47 mol/L and 3.0% respectively. Flow rate of carrier and reductant was 3.0 mL/min.

3.2.9 Optimization of Electrical Heater Temperature

In this study, a lab-made resistively heated ceramic heater was used in order to heat the quartz T-tube atomizer to the atomization temperature. In order to control the temperature of the heater, a thermocouple was placed inside the ceramic part so that its tip was in contact with the quartz tube near its conjunction with the inlet arm.

Throughout this part of the study, maximum temperature of the heater was set by the help of a temperature controller to 880, 930, 980 and 1030 °C. Temperature of the heater fluctuates between the maximum temperature set and 30 °C below the maximum temperature due to the technical restrictions of the temperature controller. As can be expected, signal heights decrease with decreasing heater temperature due to decreasing atomization efficiency inside the QTA. After a certain temperature,

there was no significant improvement in analytical signal with increasing heater temperature. Thus, in order not to damage the ceramic part of the heater with higher temperatures, 980 °C was used as the optimum maximum temperature for electrical heater. Signals versus applied furnace temperature are given in Figure 31.

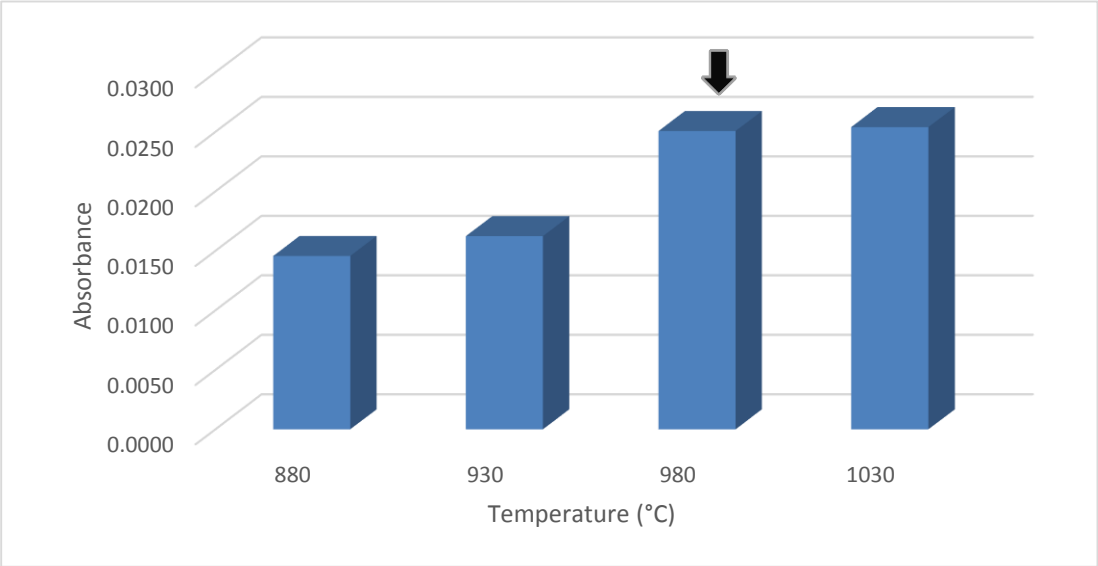

Figure 31 Effect of electrical heater temperature on the analytical signal of 1.0 mg/L In prepared in 0.47 mol/L HCl.

Carrier and reductant flow rate was 3.0 mL/min with concentrations 0.47 mol/L and 3.0% respectively. Oxygen was introduced for 60 s with 80 mL/min flow rate. Argon flow rate was set as 300 mL/min.

In order to measure the temperature profile inside QTA, maximum temperature of the electrical heater was set to 980 °C and a second thermocouple was placed at different locations in the QTA. As seen in
Figure **32** and Figure 33, temperature of the measurement zone reaches to 920 °C at the center of QTA.

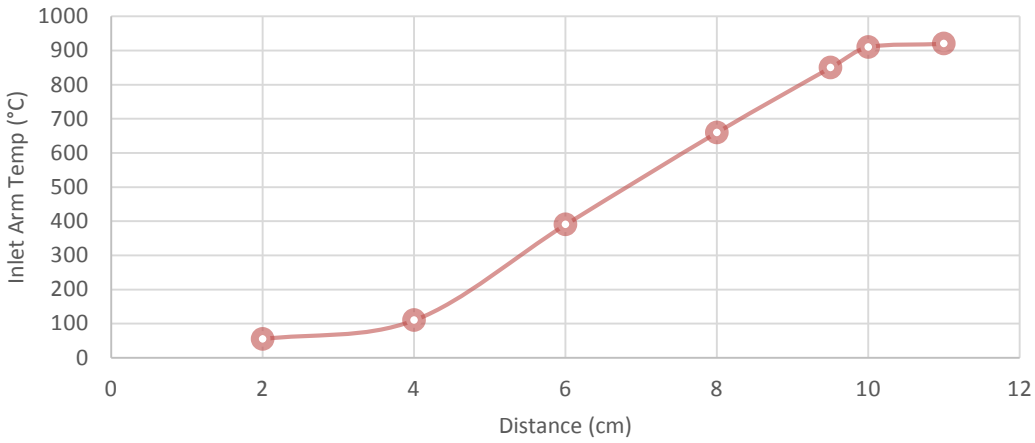

Figure 32 Temperature profile of inlet arm of the quartz T-tube atomizer.
0 cm represents the beginning of inlet arm and 9.5 cm represents the junction point of optical arm and inlet arm of the QTA.

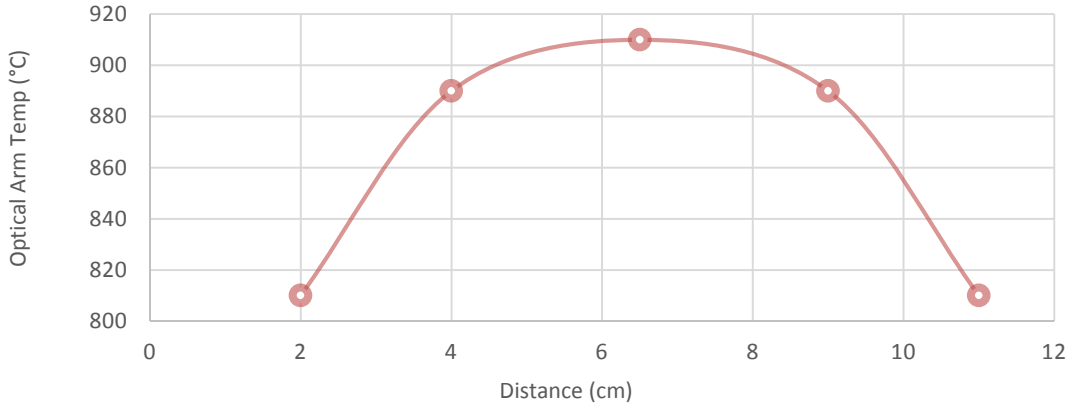

Figure 33 Temperature profile of optical arm of the quartz T-tube atomizer.
Left end is accepted as the beginning (0 cm) for the 13.5 cm optical arm of the QTA.

3.2.10 Optimization of Oxygen Introduction Position

In order to estimate the place on the quartz surface where indium volatile species are trapped, position for introduction of oxygen gas is important since it directly affects temperature profile inside the inlet arm of QTA. Trapping of the volatile species directly depend on the temperature profile of the surface because species are adsorbed to the surface in certain temperature ranges and desorbed when the surface temperature is heated to sufficient temperatures.

In this part of the study, the capillary tube used for oxygen introduction was positioned in different places of the inlet arm of QTA. Starting from the junction point between optical and inlet arms of the QTA, the quartz capillary was moved to 5.1, 8.5, 17.0 and 25.5 mm away from the junction point. It is observed that the analytical signal increased slightly with increasing distance from the junction point and at 17 mm distance, the signal heights reached to the highest value. At 25.5th mm, signal heights were decreased. If the capillary was moved further, oxygen back flow through the GLS caused small explosions inside GLS which interrupts the analytical signal. Optimum distance was therefore accepted as 17.0 mm. Results are illustrated in Figure 34.

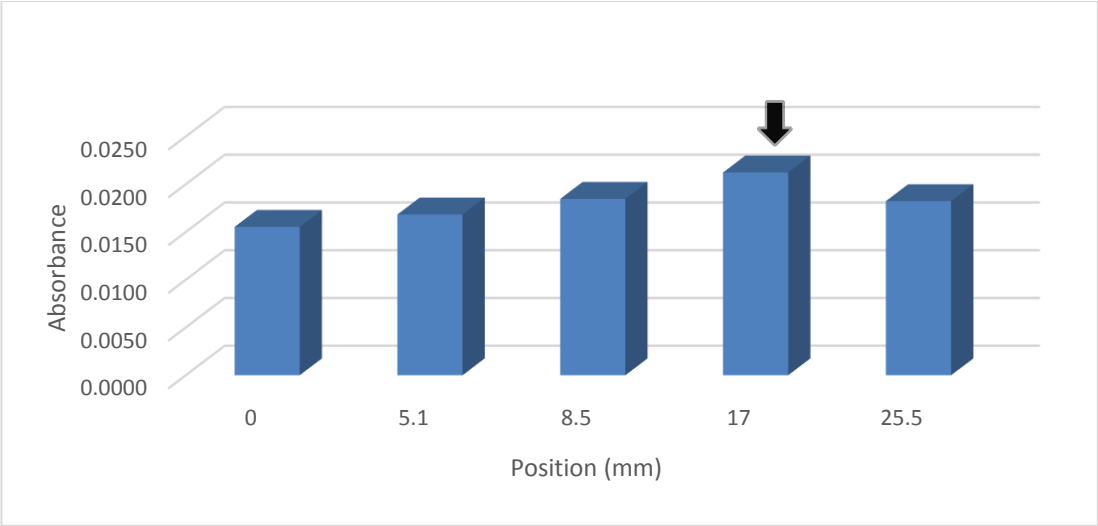

Figure 34 Effect of oxygen introduction position on the analytical signal of 1.0 mg/L indium standard solution prepared in 0.47 mol/L HCl.

With increasing available surface by increasing the distance of the capillary from the junction point, trapped species are increased and thus, signal heights were expected to be increased. It is observed throughout this optimization that, even when capillary was positioned on the junction point of the inlet and optical arms, there was not a dramatic decrease in the signal height. On the other hand, there was slight increase in the signal heights with increasing distance from the junction point. It can be concluded from this observation that, trapping of the volatile species occurs mostly inside the optical arm of QTA and a small proportion of the species are trapped inside the inlet arm. Another possibility is that, trapped species are increased with increasing distance but since the temperature gradient was changed with changing the position of mini flame, some of the trapped species could not be revolatilized and so, they were not able to reach to the measurement zone.

3.2.11 Effects of Enhancement Reagents

Vapor generation method of In has low sensitivity, compared to the conventional hydride forming elements. This makes usage of a proper enhancement reagent crucial. Possible effects of EDTA, ruthenium acetyl acetonate, 8-hydroxy quinolone, dithizone, TiO_2, rhodamine 6G and 8-mercaptoquinoline to the analytical signal of In were examined.

1.0 mg/L In solutions were prepared in 0.47 mol/L HCl. EDTA was added to the solution to get a final concentration of 0.1% (w/v). Analytical signal heights of 1.0 mg/L In solution in 0.47 mol/L and that of 1.0 mg/L In solution in 0.47 mol/L HCl and 0.1% EDTA (w/v) were compared. No significant difference was observed between the two signal heights. It is an expected result because of the pH of the sample solution. HCl concentration was optimized as 0.47 mol/L and this makes pH of the solution less than 0.5. However, to form In-EDTA complex in a satisfactory level, pH should be arranged as more than 1.0 (Skoog et al., 2004).

With the similar procedure with EDTA, 8-hydroxy quinolone, 8-mercapto quinolone and rhodamine 6G were tested as enhancement reagents. Analytical signals of 1.0 mg/L In solutions prepared in 0.47 mol/L HCl and 10 mg/L enhancement reagents were compared with that of 1.0 mg/L In solution prepared in 0.47 mol/L HCl. No significant difference was observed.

In order to increase VG efficiency of indium, ruthenium acetyl acetonate was also tested as an enhancement reagent, 100 mg ruthenium acetyl acetonate was weighed and placed right after the mixing point of sample solution and reducing agent inside a sag in form of a plastic net in the flow system. By this way, the reaction between the analyte and reducing agent took place on the surface of the ruthenium acetyl acetonate crystals in order to check whether ruthenium acetyl acetonate catalyzes the reaction or not. With this modification, about 1.2 times higher signal heights were achieved. However, ruthenium acetyl acetate is transported with the solution through GLS, making the linear range and calibration studies impracticable.

With the same procedure with ruthenium acetyl acetonate, dithizone and TiO_2 was tested to increase signal heights. However, no significant difference was observed in the signal heights of 1.0 mg/L In standard solution.

Results of the enhancement studies are summarized in Figure 35 and Table 9.

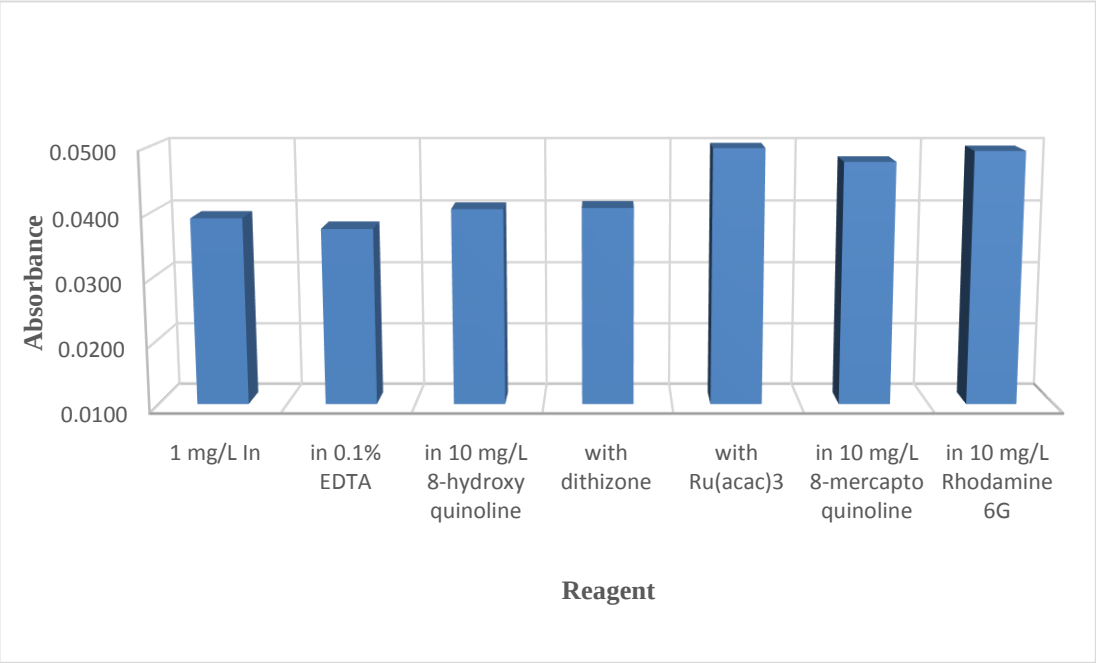

Figure 35 Effects of enhancement reagents on the flow injection VGAAS signal of 1.0 mg/L In solution prepared in 0.47 mol/L HCl.
Carrier liquid and 3.0% (m/v) $NaBH_4$ were sent with the flow rate of 3.0 mL/min. Ar flow rate was set as 300.0 mL/min and 1.0 mL sample loop was used for sample introduction. Oxygen flow rate was 80.0 mL/min and collection time was set to 60 s.

Optimized parameters are given in Table 8. Enhancement factors by means of characteristic concentrations obtained with several reagents are summarized in Table 9.

Table 8 Optimized parameters for FI-VGAAS system coupled with quartz trap.

Parameter	**Optimum Value**
Ar flow rate	300 mL/min
$NaBH_4$ concentration	3.0% (w/v)
NaOH concentration	0.3% (w/v)
HCl concentration	0.47 mol/L
$NaBH_4$ and carrier liquid flow rates	3.0 mL/min
Sample loop volume	1000 μL
Oxygen flow rate	80.0 mL/min
Oxygen introduction position (from the connection point of horizontal and optical arm)	17 mm
Collection time	60 s
Electrical Heater Temperature	980 °C

Table 9 Enhancement factors based on characteristic concentrations with several reagents.

Sample	Enhancement
1.0 mg/L In	1
1.0 mg/L In + 0.1% EDTA	0.96
1.0 mg/L In + 10 mg/L 8-hydroxy quinolone	1.04
1.0 mg/L In + Dithizone	1.04
1.0 mg/L In + Ruthenium acetyl acetonate	1.27
1.0 mg/L In + 8-mercapto quinoline	1.22
1.0 mg/L In + Rhodamine 6G	1.26
1.0 mg/L In + Titanium Dioxide	1.07

3.2.12 Linear Ranges and Calibration Plot

Various concentrations of indium standard solutions from 0.5 to 10.0 mg/L were used for the calibration studies. Calibration plot was linear between 0.5 and 5.0 mg/L concentrations. A 41 µg/L detection limit, which is described as 3 times the standard deviation of six replicate measurements of 0.5 mg/L standard solution over the slope of the calibration line was achieved. Limit of quantitation was calculated as 138 µg/L. Analytical figures of merit are summarized in Table 10 and comparison with the other studies conducted for indium determination are summarized in Calibration data are given in Figure 36 and Figure 37.

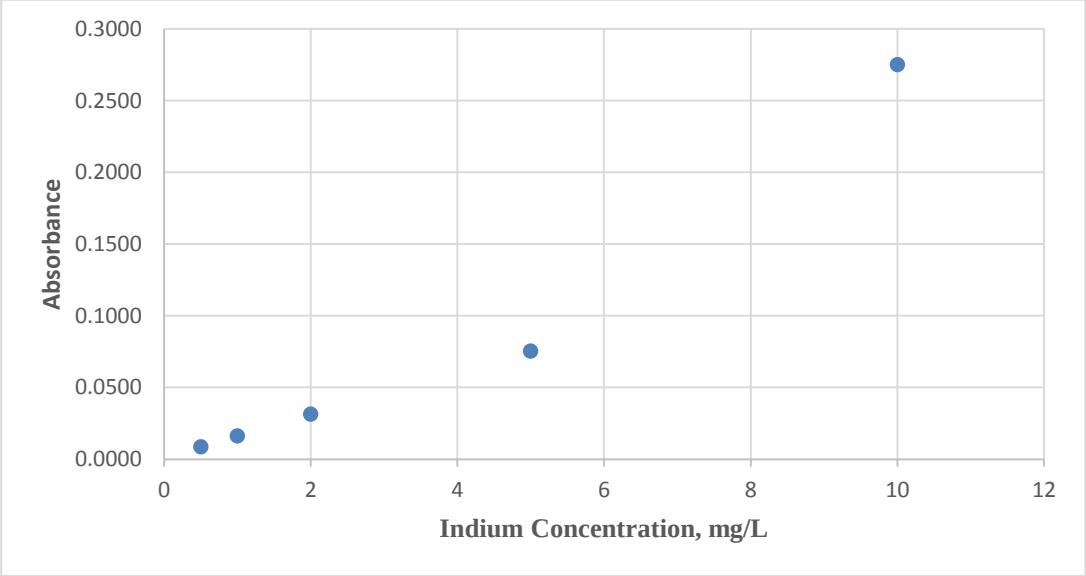

Figure 36 Calibration plot of flow injection VGAAS signals of indium standard solutions with concentrations ranging from 0.5 to 10.0 mg/L.
Solutions were prepared in 0.47 mol/L HCl. Argon, oxygen, carrier solution and reductant flow rates were set to 300, 80, 3.0 and 3.0 mL/min, respectively. Reductant concentration was 3.0% (w/v). Collection time was 60 s.

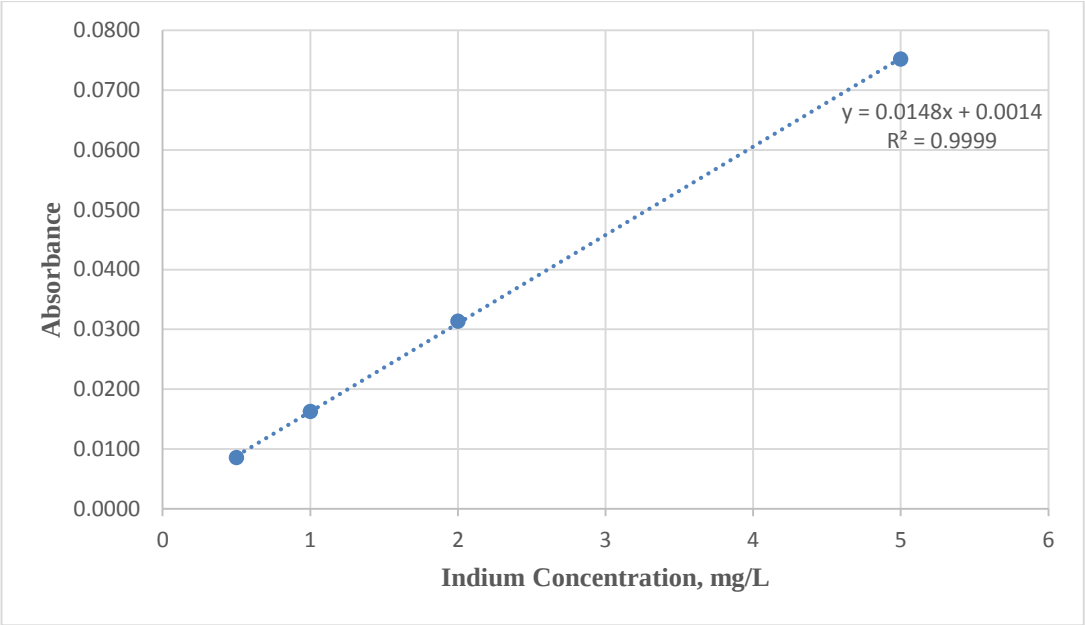

Figure 37 Calibration plot of flow injection VGAAS signals of indium standard solutions with concentrations ranging from 0.5 to 5.0 mg/L.

Solutions were prepared in 0.47 mol/L HCl. Argon, oxygen, carrier solution and reductant flow rates were set to 300, 80, 3.0 and 3.0 mL/min, respectively. Reductant concentration was 3.0% (w/v). Collection time was 60 s.

Table 10 Analytical figures of merit of flow injection VGAAS system**.** Parameters are given in Table 8.

Analytical Figure of Merit	**Value**
Limit of Detection, LOD, 3s/m (N=6) µg/L	41
Limit of Quantification, LOQ, 10s/m (N=6) µg/L	138
Characteristic Concentration, C_0, µg/L	113
Precision, % RSD (N=6) for 1.0 mg/L In	4.9

Table 11: Detection limits in this studiy and those in the literature

Reference	Method	LOD (µg/L)	C_0 (µg/L)	m_0 (µg)	%RSD
This study	FI-VGAAS	41	113	0.113	4.9
(Busheina & Headridge, 1982)	HGAAS	-	-	0.3	-
(Yan et al., 1984)	HGAAS	-	-	0.13	8.5
(Li & Liao, 1993)	HG-ETAAS	-	-	0.00063	-
(Wei et al., 1994)	ETAAS, Preconcentration	0.025	-	-	5.0
(Acar et al., 2000)	ETAAS	4.0	-	0.00004	-
(Dash et al., 2006)	ETAAS	40	-	-	-
(Matusiewicz & Krawczyk, 2007)	HG-ETAAS	6.3	-	-	-
(Matusiewicz & Krawczyk, 2007)	IAT-FAAS	10.0	-	-	-
(Matusiewicz & Krawczyk, 2007)	HG-IAT-FAAS	0.60	-	-	4.4
(Arslan et al., 2011)	SQT-FAAS	600	-	-	-
(Arslan et al., 2011)	SQT-AT-FAAS	2.60	-	-	-

3.3 Investigation of Memory Effect

This part of the study consists of 4 different parts. Aim of this study was to investigate the source of memory effect that results in high blank signals. In the first part, system was saturated with continuous flow introduction of 10.0 mg/L indium standard solution, for 5 minutes using conditions summarized in Table 8. In the saturation period, no oxygen was introduced into the system as an exception from those conditions. Blank signal was obtained with the flow injection procedure described in Experimental part after the saturation period. An example of a blank signal is given in Figure 38. Blank signal was high as it is expected.

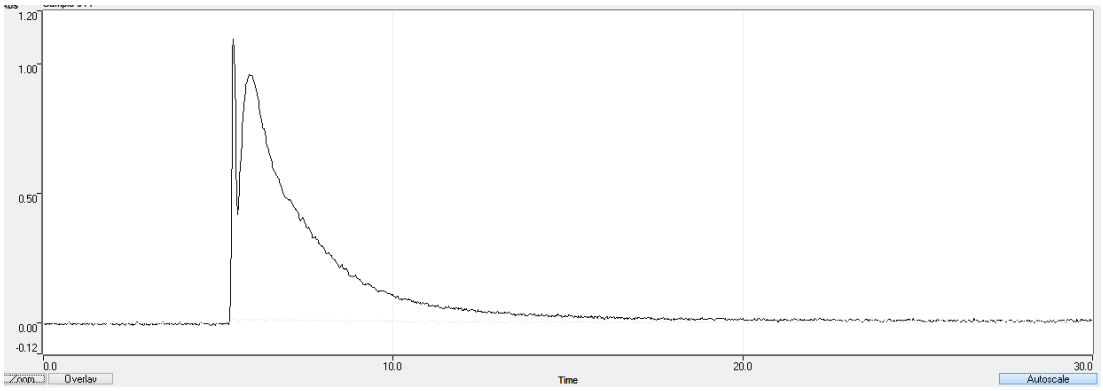

Figure 38: Investigation of memory effect. Blank signal after saturation of the system with 10.0 mg/L Indium standard solution for 5 minutes.

In order to see whether indium species adsorbed on the surface of GLS contributes to the high blank signals or not, GLS was removed from the system and a new GLS was connected to the system. The new GLS was cleaned in 10 % (v/v) nitric acid solution for 24 hours and in 10% hydrofluoric acid solution for 5 minutes before use. Blank signal was obtained from the system after changing the GLS. As shown in Figure 39, an important decrease in the signal heights were observed after removing the GLS

from the system. This proves that GLS contributes to the memory effect in a remarkable amount.

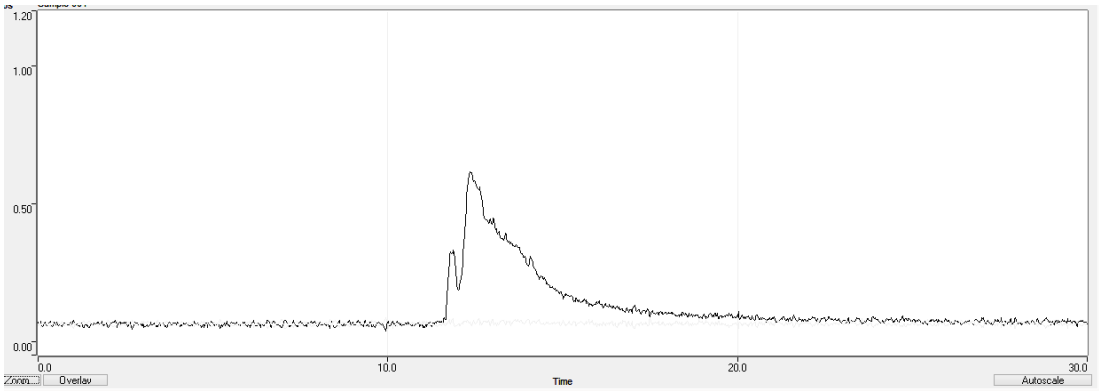

Figure 39: Investigation of memory effect. Blank signal after changing GLS.

Further manipulations on the system were put into practice. Tubing that connect GLS to the QTA were removed and changed with new ones. Decrease in the blank signals was observed. Lastly, QTA was removed from the system and a new QTA was connected. With the change of QTA, heights of the blank signals decreased in the order of 0.0080 absorbance, which was not further decreased throughout this study. Signals after removal of tubing and QTA are shown in Figure 40 and Figure 41.

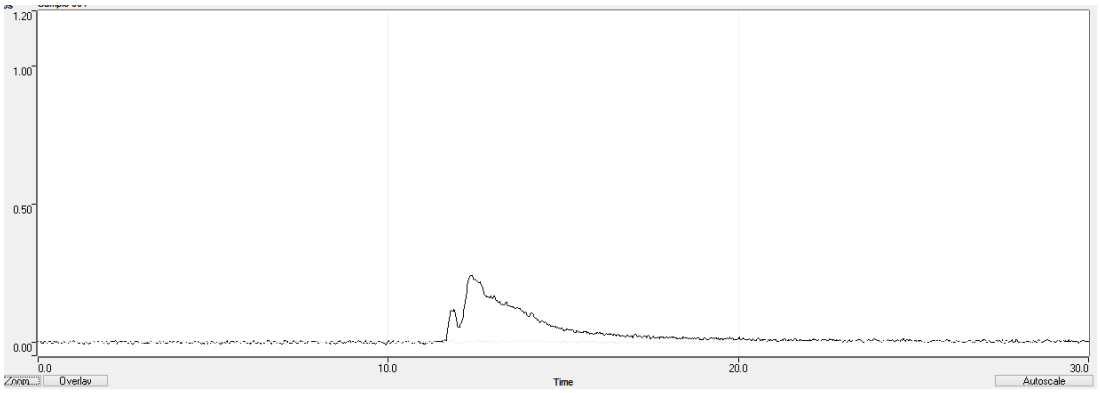

Figure 40: Investigation of memory effect. Blank signal after changing tubing connecting GLS and QTA.

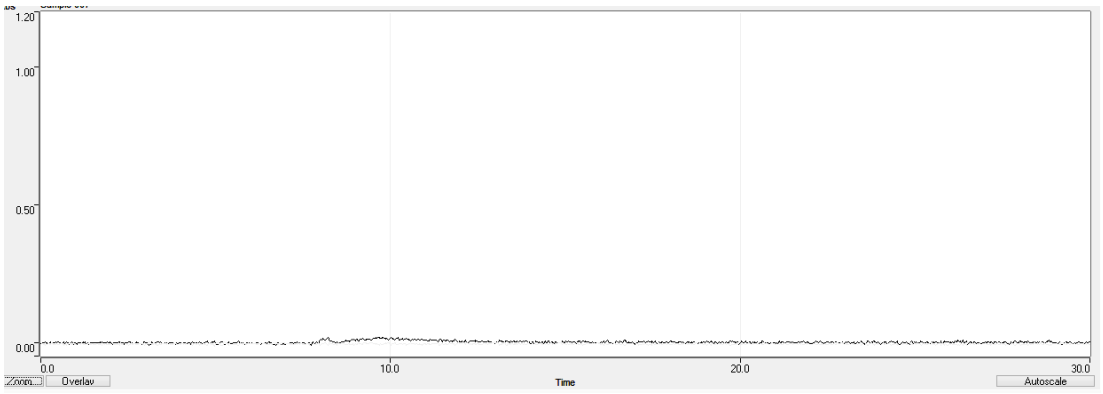

Figure 41: Investigation of memory effect. Blank signal after changing QTA.

3.4 Waste Analysis and Efficiency

In this part of the study, 10.0 mg/L standard solution of indium prepared in 0.47 mol/L HCl was used. With the optimized parameters of flow injection VGAAS system summarized in Table 8, waste solutions were picked up and determination of indium in waste solutions were carried out by ETAAS. Standard solutions for the study was prepared using waste solution picked up using 0.47 mol/L HCl and 3.0 % (w/v) $NaBH_4$. All these standard solutions were diluted in a 1/20 ratio in order to minimize the interferences arising from matrix. Calibration plot is given in Figure 42.

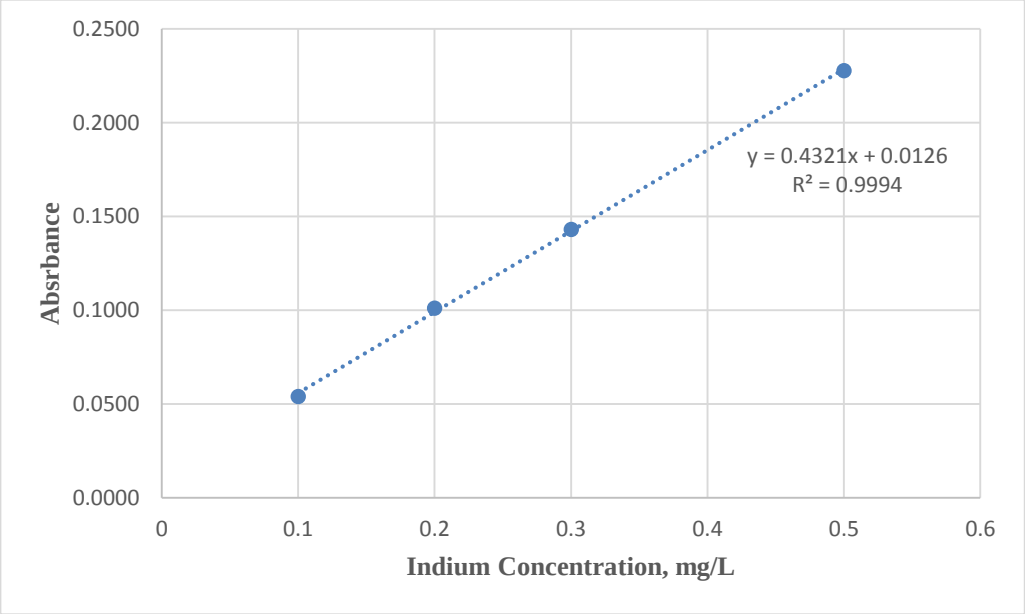

Figure 42 Calibration plot of ETAAS signals of indium standard solutions with concentrations ranging from 0.1 to 0.5 mg/L.

Solutions were prepared by addition of appropriate volumes of 10.0 mg/L indium solution prepared in 0.47 mol/L HCl to the waste solutions picked up from the reaction between 0.47 mol/L HCl and 3.0(w/v) $NaBH_4$, and dilution with appropriate amount of de-ionized water.

Waste solution picked up using 10.0 mg/L indium solution as analyte in 0.47 mol/L HCl and 3.0% (w/v) $NaBH_4$ as reducing agent was found to be containing 8.95 mg/L indium, meaning that at least 89.5% of the analyte is removed from the system and cannot reach to the atomization zone. Volatile species of indium is reported in the literature as unstable and prone to decomposition. Thus, they can be adsorbed on the walls of QTA and tubing between GLS and QTA. Moreover, some amount of indium can be retained on the walls of GLS. As a result, vapor generation efficiency of indium with the system described here is equal or less than 10.5%.

3.5 Nature of Volatile Indium Species

In order to investigate the nature of the volatile indium species, a syringe filter with 0.2 μm pore size was placed between GLS and QTA, as illustrated in Figure 43. With 100 mL/min Ar flow rate, 60 s collection period with 80 mL/min oxygen flow rate, 1.0 mL/min carrier acid and reductant reagent flow rates, and 1.0 mL loop volume, behavior of indium volatile species was similar with that of SbH_3. Both indium and antimony volatile species passed through the filter and reached to the QTA and analytical signal of both antimony and indium were obtained in the presence of filter. Signals are shown in Figure 44 and Figure 45.

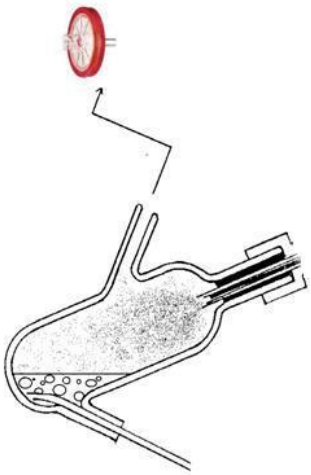

Figure 43 0.2 µm pore size syringe filter placed between GLS and QTA.

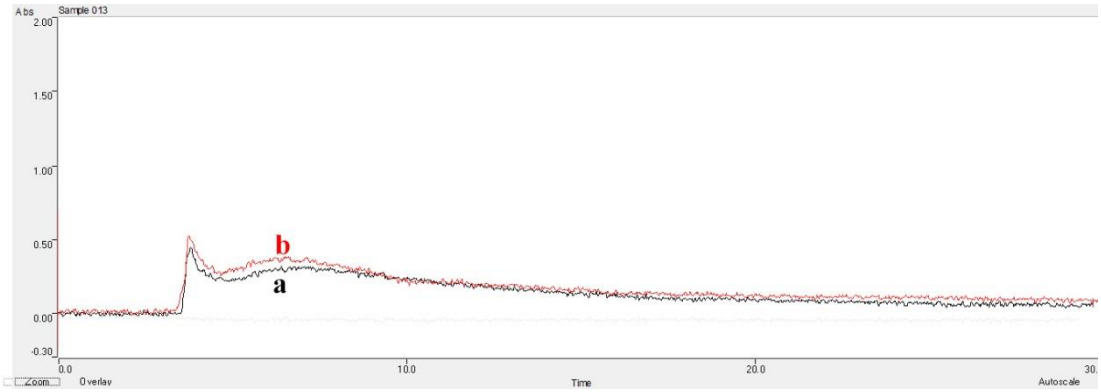

Figure 44 Analytical signal of 0.025 mg/L Sb solution prepared in 0.47 mol/L HCl a) in the presence of 0.2 µm pore size filter, b) Without filter.

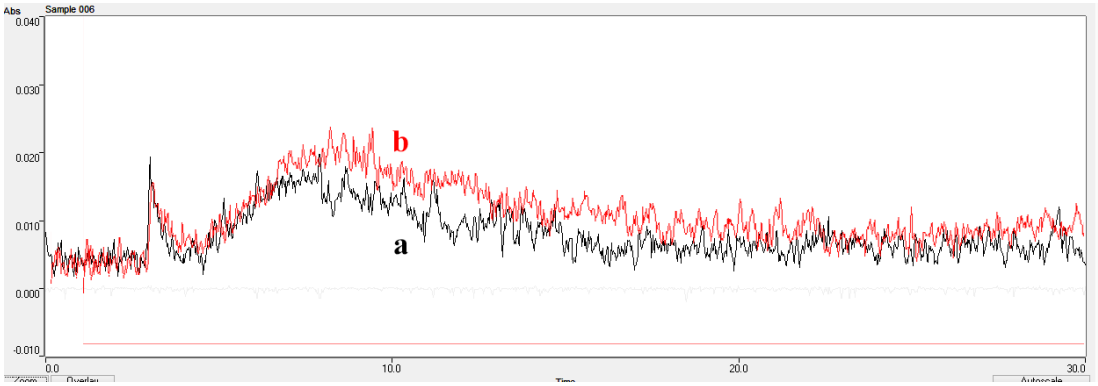

Figure 45 Analytical signal of 2.0 mg/L In solution prepared in 0.47 mol/L HCl a) in the presence of 0.2 µm pore size filter, b) Without filter.

Nature of the trapped species on the quartz surface were also investigated throughout this part of the study. A 100 mg/L In solution was prepared and VGAAS procedure for indium is applied using the conditions summarized in Table 8. Differently from that conditions, injection valve was removed and sample solution was directed continuously through the system. In the precence of external oxygen, indium volatile species were trapped for 30 minutes. 4 square quartz plates with 12 mm edge were placed on the right side of the QTA, as shown in Figure 46 in order to supply a quartz trapping surface that is compatible with XRD sample holder. After 30 minutes trapping period, quartz plates were analyzed using an XRD spectrometer. As a result of this part of the study, trapped species on the quartz surface shows a characteristic spectrum, implying a crystal structure. As it is shown in Figure 47, Figure 48, Figure 49, Figure 50 and Figure 51, amount of trapped species decreases with increasing distance from the center of optical arm to the edges and the spectrum of quartz plate numbered as 4 is about the same with the heated blank plate. Identification of the coumpound(s) giving the spectrum is not achieved and will be done as a future work.

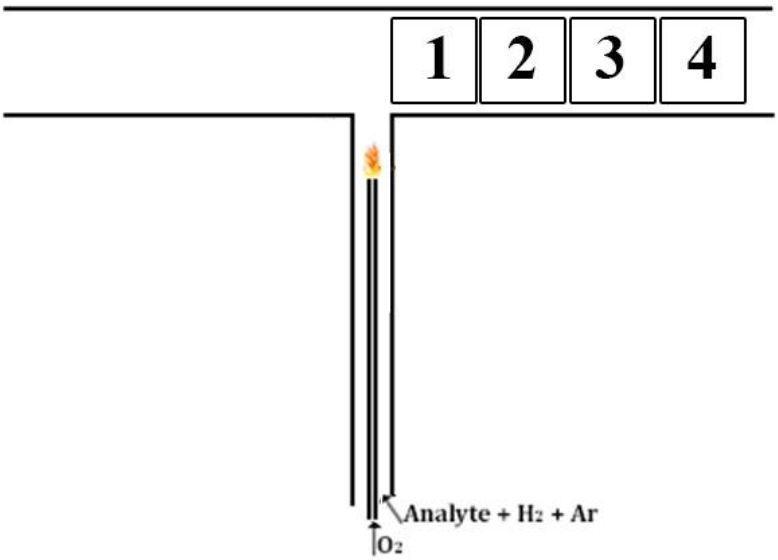

Figure 46: Investigation of the nature of trapped species. 4 quartz plates are positioned inside the QTA.

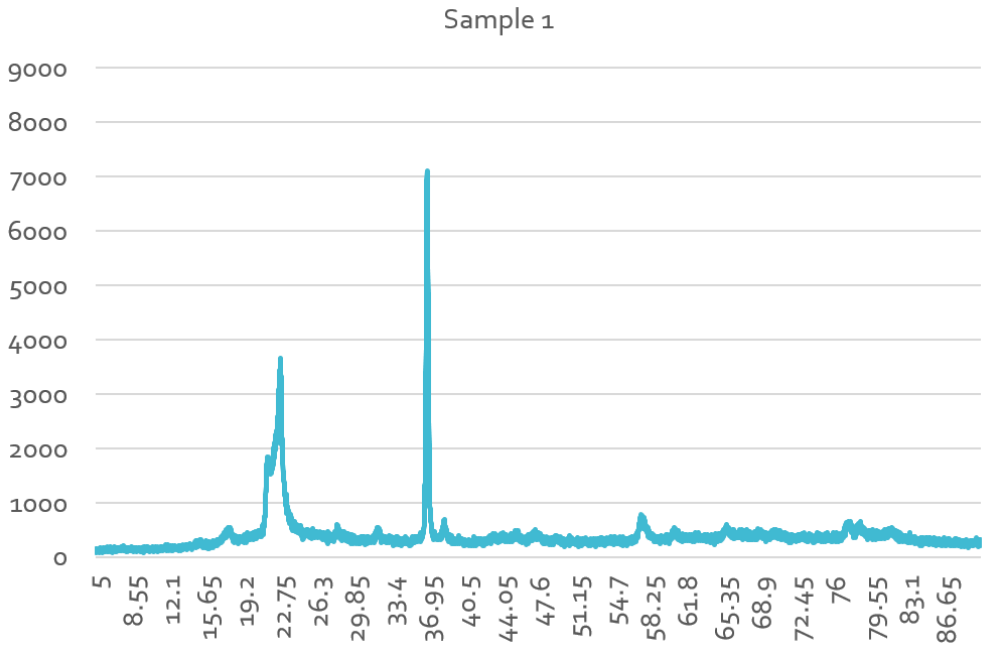

Figure 47: Investigation of the nature of trapped species. XRD spectrum of quartz plate 1.

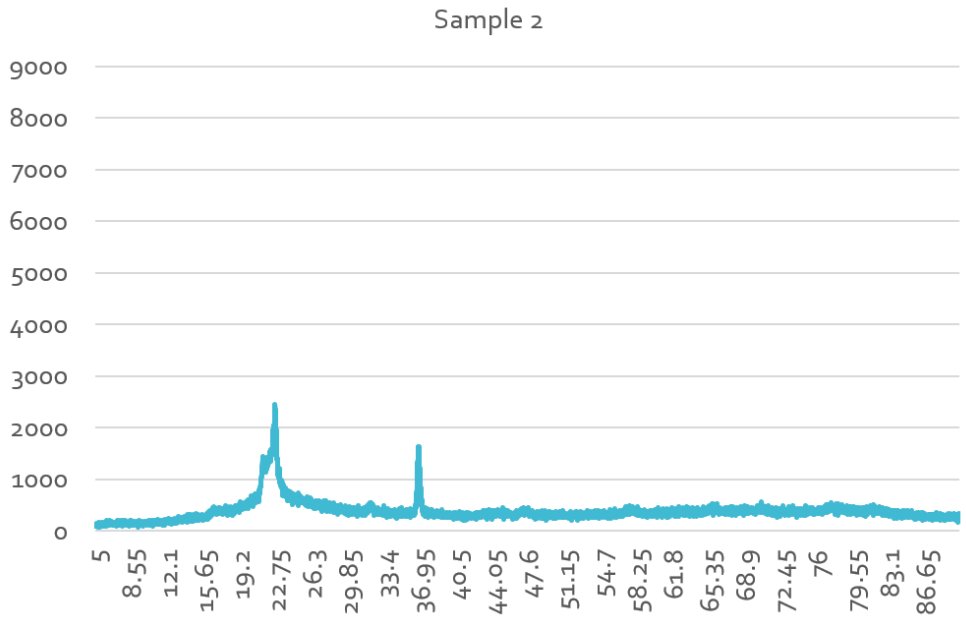

Figure 48: Investigation of the nature of trapped species. XRD spectrum of quartz plate 2.

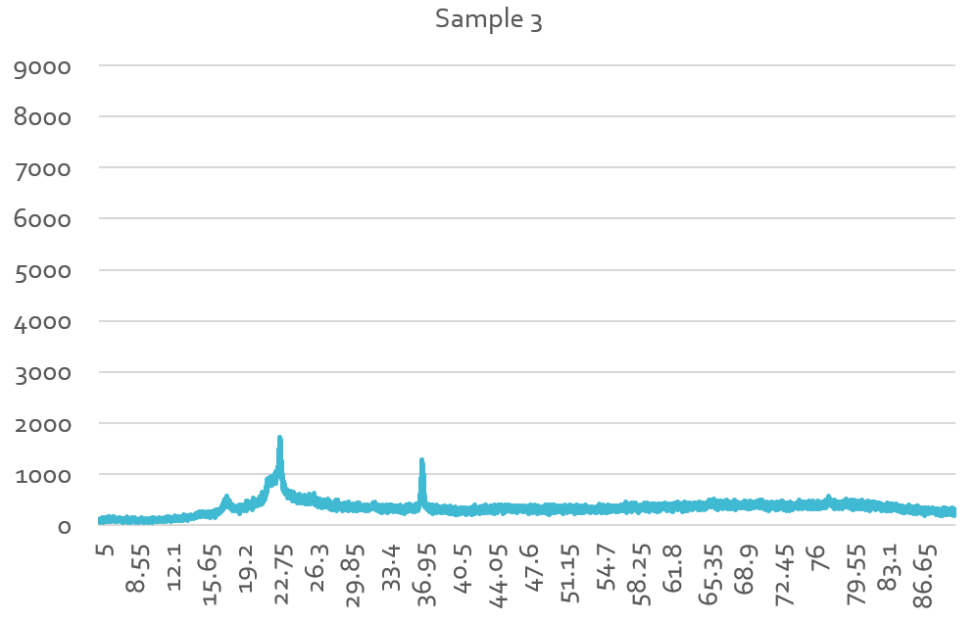

Figure 49: Investigation of the nature of trapped species. XRD spectrum of quartz plate 3.

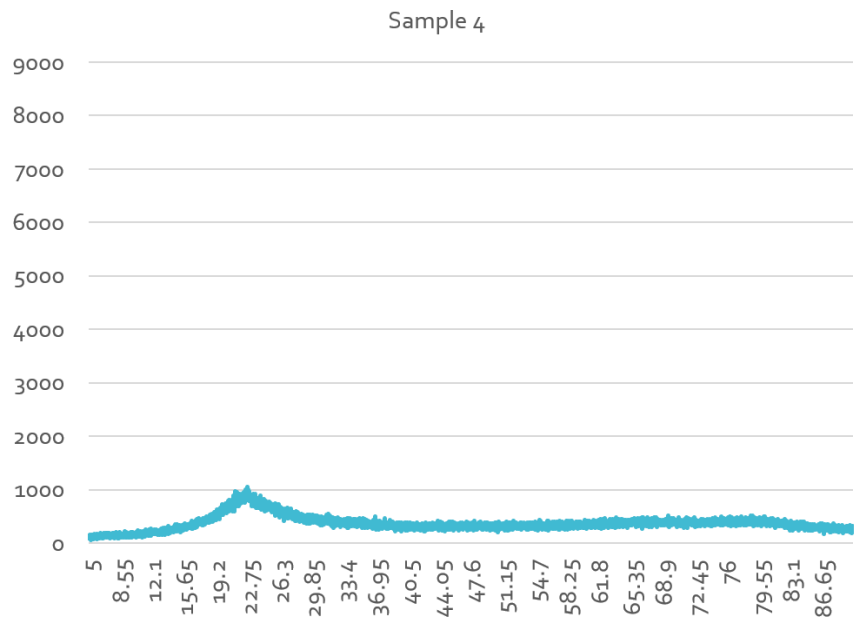

Figure 50: Investigation of the nature of trapped species. XRD spectrum of quartz plate 4.

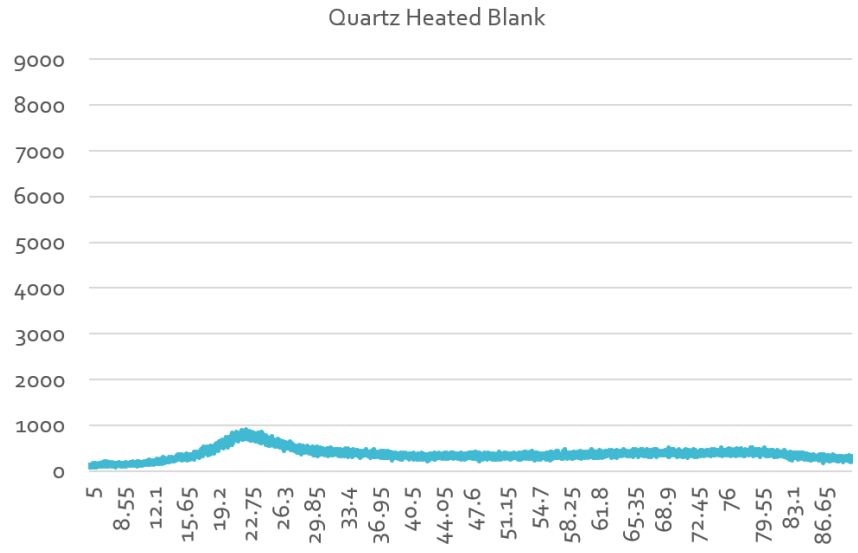

Figure 51: Investigation of the nature of trapped species. XRD spectrum of blank quartz plate heated to 980 °C.

3.6 Photochemical Vapor Generation

For generation of volatile species for indium, photochemical vapor generation procedure was also tested. The system was prepared with optimum conditions for selenium which were reported by Sturgeon and his collaborators (Xuming et al., 2003). A successive signal with 6.5 μg/L characteristic concentration was gained with 0.2 mg/L selenium standard solution prepared in 10% (v/v) acetic acid. The same system with same conditions was tested for 5.0 mg/L indium standard solution prepared in 10% (v/v) acetic acid. However, no analytical signal was observed in AAS. The same test was conducted for indium standard solutions prepared in formic acid and propionic acid. However, no signal was obtained in all cases.

After this trial, waste solution in this system was collected from GLS and analyzed with ICPOES. Indium standard solutions were prepared in 10% (v/v) acetic acid and concentration of indium in waste solutions were determined using ICPOES instrument.

As a result, it was observed that almost all indium was transported to the waste. It can be concluded from this test that, indium vapor generation was not achieved and no indium volatile species are transported through the measurement zone.

CHAPTER 4

CONCLUSIONS

The main purpose of this study was to develop an alternative analytical method for determination of indium with a low detection limit.

In order to overcome the memory effect problem in conventional continuous flow system, GLS was replaced by a smaller one and reaction coil was removed in order to separate the volatile species right after the formation. By this way, decomposition of volatile species due to their unstable nature was minimized. In order to collect the volatile species on the measurement zone, hydrogen produced was consumed by a flow of oxygen inside the inlet arm of QTA. Atomization of volatile species were minimized since hydrogen did not reach to the measurement zone and as a result, volatile species were collected on the measurement zone. Optimization of parameters were achieved and as a result, a detection limit of 41 μg/L was achieved with 4.9% RSD for 1.0 mg/L. This limit of detection was not as low as expected. However, reproducibility of the system was enhanced and about a 50 fold increment in the sensitivity was achieved compared to conventional FAAS. In order to enhance the sensitivity, several enhancement reagents were tried but no achievement was obtained by means of characteristic concentration.

After optimization and calibration studies, behavior of indium volatile species and nature of quartz trap was investigated. Sources of memory effect associated with determination of indium in flow injection system coupled with quartz trap was investigated. As a conclusion of third part of the study, GLS was observed as the most important source of memory effect. Moreover, QTA was another contributor to the memory effect.

Chemical vapor generation efficiency was found to be 10.5% for indium during the fourth part of the study. Considering the transportation efficiency and unstable nature of the volatile species of indium, it can be concluded that even less than 10.5% of the analyte reaches to the measurement zone. This is concluded as the main reason of poor detection limits in determination of indium.

Indium volatile species are observed to be passing through a 0.2 μm pore size filter, as it is the case for SbH_3. As a conclusion of this part, it can be stated that indium transportable species does not show a nanoparticle behavior as it is the case for silver (Musil et al., 2011) and gold (Arslan et al., 2011). Moreover, indium species were collected on quartz plate surfaces and analyzed using an XRD spectrometer in order to get molecular information about trapped species of indium. As a result of this part, species trapped on quartz surface were observed to show a characteristic XRD spectrum. However, these species could not be identified in this part of the study and left as a future work.

The last part of the study was a search for an alternative vapor generation system for indium. For this purpose a UV reactor was designed and tested for selenium element. Characteristic concentrations comparible with the ones in the literature was obrained. Then, the same design was tested for indium with the same operational conditions. However, no analytical signal was obtained in this study. In addition, different organic acids such as formic acid and propionic acid were tested besides acetic acid. However, no achievement was obtained. Then, waste solutions of this system were analyzed using an ICPOES instrument and it was concluded that no volatile indium species reach to the measurement zone with this design.

As a general conclusion, although analttical figures of merit were not very competitive, a thorough characterization was completed regarding the quartz trap using hydride generation AAS. Surface characterization requires further work.

REFERENCES

Acar, O., Türker, R. A., & Kılıç, Z. (200). Determination of bismuth, indium and lead in spiked sea water by electrothermal atomic absorption spectrometry using tungsten containing chemical modifiers. *Spectrochim. Acta B. 55* , 1635-1641.

ACGIH. (2001). *Documentations of the Threshold Limit Values and Biological Exposure Indices.* Cincinnati, Ohio: American Conference of Governmental Industrial Hygienists.

Alfantazi, A. M., & Moskalyk, R. R. (2003). Processing of indium: a review. *Minerals Engineering*, 687-697.

Arslan, Y., Kendüzler, E., & Ataman, O. Y. (2011). Indium determination using slotted quartz tube-atom trap-flame atomic absorption spectrometry and interference studies. *Talanta*, 432-436.

Asami, T., Mizui, C., Shimada, T., & Kubota, M. (1996). Determination of Thallium in Solids by Flame Atomic Absorption Spectrometry. *Fresen. J. Anal. Chem., 356*, 348-351.

Ataman, O. Y. (2008). Vapor Generation and Atom Traps: Atomic Absorption Spectrometry at the ng/L Level. *Spectrochim. Acta, Part B, 63*, 825-834.

Bakırdere, S., Aydın, F., Bakırdere, E. G., Titretir, S., Akdeniz, İ., Aydın, I., Yıldırım, E., Arslan, Y. (2011). From mg/kg to pg/kg Levels: A Story of Trace Element Determination: A Review. *Appl. Spectrosc. Rev., 46*, 38-66.

Barbalace, K. (2013, 10 13). *Periodic Table of Elements*. Retrieved from Environmental Chemistry.com: http://environmentalchemistry.com/yogi/periodic/In.html on 02.02.2014

Bhuiyan, A. G., Hashimoto, A., & Yamamoto, A. (2003). Indium nitride „InN…: A review on growth, characterization, and properties. *J. Appl. Phys.*, 2779-2804.

Bleshinsky, S. V., & Abramova, V. F. (1958). Химия индия. *Frunze*, 252.

Blumenthal, B., Sellers, K., & Koval, M. (2006). Thallium and Thallium Compounds. *Kirk-Othmer Encycl. Chem. Technol.*, *23*, 1-16.

Boothroyd, A. I. (2006). Heavy elements in stars. *Science 314*, 1690-1691.

Broekaert, J. A. (2005). *Analytical Atomic Spectrometry with Flames and Plasmas* (Second, Completely Revised and Extended Edition ed.). Weinheim: WILEY-VCH.

Busheina, I. S., & Headridge, J. B. (1982). Determination of indium by hydride generation and atomic-absorption spectrometry. *Talanta 29*, 519-520.

Campbell, A. D. (1992). A Critical Survey of Hydride Generation Techniques in Atomic Spectroscopy. *Pure Appl. Chem., 64*, 227-244.

Cantle, J. E. (1982). *Atomic Absorption Spectrometry.* Amsterdam: ELSEVIER SCIENTIFIC PUBLISHING COMPANY.

Dash, K., Thangavel, S., Chaurasia, S. C., & Arunachalam, J. (2006). Determination of indium in high purity antimony by electrothermal atomic absorption spectrometry (ETAAS) using boric acid as a modifier. *Talanta 70*, 602-608.

Dědina, J. (2010). Generation of Volatile Compounds for Analytical Atomic Spectroscopy. *Encyclopedia of Analytical Chemistry*, DOI:10.1002/9780470027318.a9127.

Dedina, J., & Matousek, T. (2000). Multiple microflame—a new approach to hydride atomization for atomic absorption spectrometry. *Journal of Analytical Atomic Spectrometry, 15*, 301 - 304.

Dědina, J., & Tsalev, D. L. (1995). *Hydride Generation Atomic Absorption Spectrometry.* Chichester: John Wiley & Sons Ltd.

Downs, J. (1993). *Chemistry of Aluminium, Gallium, Indium, and Thallium.* Glasgow: Springer.

Ebdon, L., Wikinson, J. R., & Jackson, K. W. (1982). A simple and sensitive continuous hydride generation system for the determination of arsenic and selenium by atomic-absorption and atomic fluorescence spectrometry. *Anal. Chim. Acta. 136*, 191-199.

Florence, T. M. (1986). Electrochemical Approaches to Trace Element Speciation in Waters. A Review. *Analyst, 111*, 489-505.

Frech, W., & Baxter, D. C. (1996). Spatial Distributions of Non-atomic Species in Graphite Furnaces. *Spectrochim. Acta, Part B, 51*, 961-972.

Gottschling, B. C., Maronpot, R. R., & Hailey, J. R. (2001). The role of oxidative stress in indium phosphide-induced lung carcinogenesis in rats. *Toxicol. Sci. 64*, 28-40.

Hoet, P., E. De Graef, B., & Swennen. (2012). Occupational exposure to indium: What does biomonitoring tell us? *Toxicol. Lett. 213*, 122-128.

Homma, S., Miyamoto, A., Sakamoto, S., Kishi, K., Motoi, N., & Yoshimura, K. (2005). Pulmonary fibrosis in an individual occupationally exposed to inhaled indium-tin oxide. *Eur. Respir. J. 25*, 200-204.

Homma, T., Ueno, T., Sekizawa, K., Tanaka, A., & Hirata, M. (2003). Interstial pneumonia developed in a worker dealing with particles containing indium-tin oxide. *J. Occup.Health. 45*, 137.

Johansen, O., & Steinnes, E. (1976, 27). A method for the use of indium as an activable tracer in pollution studies. *The International Journal of Applied Radiation and Isotopes*, 163-167.

Keith, L. H., & Telliard, W. (1979). ES&T Special Report: Priority Pollutants: I-a Perspective View. *Environ. Sci. Technol., 13*, 416-423.

Korkmaz, D., Dedina, J., & Ataman, O. Y. (2004). Stibine preconcentration in a quartz trap with subsequent atomization in the quartz multiatomizer for atomic absorption spectrometry. *J. Anal. At. Spectrom. 19*, 255-259.

Korkmaz, D., Demir, C., Aydın, F., & Ataman, O. Y. (2005). Cold vapour generation and on-line trapping of cadmium species on quartz surface prior to detection by atomic absorption spectrometry. *J. Anal. At. Spectrom. 20*, 46-52.

Korkmaz, D., Ertaş, N., & Ataman, O. Y. (2002). A novel silica trap for lead determination by hydride generation atomic absorption spectrometry. *Spectrochimica Acta Part B 57*, 571-580.

Kratzer, J., & Dedina, J. (2005). In situ trapping of bismuthine in externally heated quartz tube atomizers for atomic absorption spectrometry. *J. Anal. At. Spectrom.*, 208-210.

Kratzer, J., & Dedina, J. (2008). Stibine and bismuthine trapping in quartz tube atomizers for atomic absorption Spectrometry. *Spectrochim. Acta. B. 63*, 843 - 849.

Kumar, A. R., & Riyazuddin, P. (2010). Chemical Interferences in Hydride-Generation Atomic Spectrometry. *Trends Anal. Chem., 29*, 166-176.

Laborda, F., Bolea, E., & Castillo, J. R. (2007). Electrochemical Hydride Generation As a Sample-Introduction Technique in Atomic Spectrometry: Fundamentals, Interferences, and Applications. *Anal. Bioanal. Chem. 388*, 743-751.

Laborda, F., Bolea, E., Baranguan, M. T., & Castillo, J. R. (2002). Hydride Generation in Analytical Chemistry and Nascent Hydrogen: When is it Going to be Over? *Spectrochim. Acta, Part B, 57*, 797-802.

Li, A., & Liao, Y. (1993). Indium Hydride Generation Atomic Absorption Spectrometry with ln Sifu Preconcentration in a Graphite Furnace Coated with Palladium. *J. Anal. At. Spectrom. 8*, 633-636.

Liao, Y.-P., Chen, G., Yan, D., Li, A.-M., & Ni, Z.-M. (1998). Investigation of Thallium Hydride Generation Using in Situ Trapping in Graphite Tube by Atomic Absorption Spectrometry. *Anal. Chim. Acta, 360*, 209-214.

Lin, T. S., & Nriagu, J. O. (1999). Thallium Speciation in River Waters with Chelex-100 Resin. *Anal. Chim. Acta, 395*, 301-307.

L'vov, B. L. (2005). Fifty Years of Atomic Absorption Spectrometry. *J. Anal. Chem., 60*, 382-392.

Matusiewicz, H., & Krawczyk, M. (2007). Hydride Generation-in situ Trapping-flame Atomic Absorption Spectrometry Hybridization for Indium and Thallium Determination. *J. Braz. Chem. Soc. 18*, 304-311.

Menemenlioğlu, İ., Korkmaz, D., & Ataman, O. Y. (2007). Determination of antimony by using a quartz atom trap and electrochemical hydride generation atomic absorption spectrometry. *Spectrochimica Acta Part B 62*, 40-47.

Murphy, M. D., & Mikolajczak, C. (2013, 10 13). *Sustainability of indium and Gallium Supplies in the Face of emerging Markets*. Retrieved from Globalspec.com: http://www.globalspec.com/Indium/ref/SustainabilityofIndiumandGallium.pdf

Musil, S., Kratzer, J., Vobecký, M., Benada, O., & Matoušek, T. (2010). Silver Chemical Vapor Generation for Atomic Absorption Spectrometry: Minimization of Transport Losses, Interferences and Application to Water Analysis. *J. Anal. At. Spectrom., DOI: 10.1039/c0ja00018c*.

Nagano, K., T. Nishizawa, Y., & Umeda. (2011). Inhalation carcinogenicity and chronic toxicity of indium-tin-oxide in rats and mice. *J. Occup. Health (53)*, 175–187.

Nostrand, D. V., Abreu, S. H., Callaghan, J. J., Atkins, F. B., Stoops, H. C., & Savory, C. G. (1988). In-111-labeled white blood cell uptake in noninfected closed fracture in humans: prospective study. *Radiological Society of North America, 167(2),* 495-498.

Omura, M., Yamazaki, K., Tanaka, A., Hirata, M., Makita, Y., & Inoue, N. (2000). Changes in the testicular damage caused by indium arsenide and indium phosphide in hamsters during two years after intratracheal instillations. *J. Occup. Health 42,* 196-204.

Pavlíčkova, J., Zbíral, J., Smatanová, M., Habarta, P., Houserová, P., & Kubáň, V. (2006). Uptake of Thallium from Naturally-Contaminated Soils into Vegetables. *Food Addit. Contam., 23,* 484-491.

Pérez-Ruiz, T., Martínez-Lozano, C., Tomás, V., & Casajús, R. (1996). Simple Flow Injection Spectrofluorimetric Method for Speciation of Thallium. *The Analyst, 121,* 813-816.

Pohl, P. (2004). Recent Advances in Chemical Vapour Generation via Reaction with Sodium tetrahydroborate. *Trends Anal. Chem., 23,* 21-27.

Reich, F., & Richter, T. (1863). Ueber das Indium. *Journal für Praktische Chemie 90,* 172-179.

Robbins, W. B., & Caruso, J. A. (1979). Development of Hydride Generation Methods forAtomic SpectroscopicAnalysis. *Anal. Chem 51,* 889-898.

Salvin, W., & Manning, D. C. (1980). The L'vov Platform for Furnace Atomic Absorption Analysis. *Spectrochim. Acta, Part B, 35,* 701-714.

Scheckel, K. G., Lombi, E., Rock, S. A., & Mclaughlin, M. J. (2004). In Vivo Synchrotron Study of Thallium Speciation and Compartmentation in Iberis Intermedia. *Environ. Sci. Technol., 38,* 5095-5100.

Shan, X.-Q., Ni, Z.-M., & Zhang, L. (1984). Application of Matrix Modification in Determination of Thallium in Waste Water by Graphite-Furnace Atomic-Absorption Spectrometry. *Talanta, 31,* 150-152.

Skoog, D. A., West, D. M., Holler, J. F., & Crouch, S. R. (2004). *Fundamentals of Analytical Chemistry.* Thomson.

Sturgeon, R. E., Guo, X., & Mester, Z. (2005). Chemical Vapor Generation: Are Further Advances Yet Possible? *Anal. Bioanal. Chem., 382,* 881-883.

Sutherland, J. K. (1971). A second occurrence of dzhalindite. *The Canadian Mineralogist 10*, 781-786.

Tadatsugu, M. (2005). Transparent conducting oxide. *Semicond. Sci. Technol. 20*, 35-44.

Taguchi, O., & Chonan, T. (2006). Three cases of indium lung. *J. Jpn. Respir. Soc. 44*, 532.

Tanaka, A., Hirata, M., Kiyohara, Y., Nakano, M., & Omae, K. (2010). Review of pulmonary toxicity of indium compounds to animals and humans. *Thin Solid Films*, 2934-2936.

Tolcin, A. C. (2010). *Mineral Commodity Summaries.* U.S. Geological Survey.

Tolcin, A. C. (2013). Indium. *USGS Mineral Commodity Summaries.*

Tsalev, D. L. (1999). Hyphenated Vapour Generation Atomic Absorption Spectrometric Techniques. *J. Anal. At. Spectrom., 14*, 147-162.

Vale, M. G., Silva, M. M., Welz, B., & Newka, R. (2002). Control of Spectral and Non-spectral Interferences in the Determination of Thallium in River and Marine Sediments Using Solid Sampling Electrothermal Atomic Absorption Spectrometry. *J. Anal. At. Spectrom., 17*, 38-45.

Virta, R. L. (2012). *U.S. Geological Survey Minerals Yearbook.* U.S. Department of Interrior.

Wei, J., Liu, Q., & Okutani, T. (1994). Determination of Trace Amounts of Indium by Graphite-Furnace Atomic Absorption Spectrometry after Preconcentration as the Acetylacetonato Complex on Activated Carbon. *Anal. Sci. 10*, 465-469.

Welz, B., & Sperling, M. (1999). *Atomic Absorption Spectrometry* (3 ed.). Weinheim: WILEY-VCH.

Wikipedia. (2008, 10 11). *AAS Block Diagram.* Retrieved from Wikipedia: http://en.wikipedia.org/wiki/File:AASBLOCK.JPG on 02.02.2014

Xu, S., Zhou, H., Du, X., & Zhu, D. (2001). Enhancement Reagents for Response Signals of Copper, Gold and Thallium in Flow Injection Vapor Generation AAS. *Chem. J. Int., 3*, 29-34.

Xuming, G., Sturgeon, R. E., Mester, Z., & Gardner, G. (2003). UV Vapor Generation for Determination of Selenium by Heated Quartz Tube Atomic Absorption Spectrometry. *Anal. Chem. 75*, 2092-2099.

Yan, D., Yan, Z., Cheng, G.-S., & Li, A.-M. (1984). Determination of Indium and Thallium by Hydride Generation and Atomic-Absorption Spectrometry. *Talanta, 31*, 133-134.

Zen, J.-M., & Wu, J.-W. (1997). Square-wave Voltammetric Stripping Analysis of Thallium(III) at a Poly(4-vinylpyridine)/mercury Film Electrode. *Electroanalysis, 9*, 302-306.

Zendelovska, D., & Stafilov, T. (2001). Extraction Separation and Electrothermal Atomic Absorption Spectrometric Determination of Thallium in Some Sulfide Minerals. *Anal. Sci., 17*, 425-428.

Zheng, W., Winter, S. M., Kattnig, M. J., Carter, D. E., & Sipes, I. G. (1994). Tissue distribution and elimination of indium in male Fischer 344 rats following oral and intratracheal administration of indium phosphide. *J. Toxicol. Environ. Health (43)*, 483-494.

Zhu, D., & Xu, S. (2000). Enhancement of Thallium Response by Flow Injection Hydride Generation AAS Using Palladium and Rhodamine B. *At. Spectrosc., 21*, 136-142.